Title

An Integrative Theory of Dark Energy, Dark Matter, and Consciousness, linking Quantum Mechanics and General Relativity.

Author: BRIAN RAMHARACKSINGH

Affiliation: Independent Research

Corresponding Author: BRIAN RAMHARACKSINGH

TRINIDAD AND TOBAGO

E-mail: drbrnsingh@gmail.com

ORCHID ID: 0009-0001-2694-5657

Abstract

The two most significant theories of the twentieth century, Quantum Mechanics (QM) and Einstein's Theory of General Relativity (GR), are currently the best explanations for our observable universe. Despite this, there are gaps in our knowledge, such as quantum gravity, dark energy, dark matter, consciousness, and the measurement problem, to name a few. The "Integrative Theory" provides a comprehensive explanation that untangles the web of these unknowns into one unified framework. This is achieved by proposing a cosmogenesis that offers solutions to the nature of dark energy, dark matter, and consciousness, demonstrating how their interactions have and can produce the standard model of particle physics of Quantum Mechanics (QM), the curved spacetime of General Relativity (GR), and the Consciousness of beings. It also resolves several other problems, such as the matter-antimatter asymmetry, the fine structure

constant, the Hubble tension, early galaxy and supermassive black hole formation, and the hard problem of consciousness. This research aims to deepen our understanding of the physical laws governing the fabric of reality.

Introduction

Physics has always been about understanding the structure and forces that govern our Universe through the interactions of energy and matter. Current estimates propose that 95% of the Universe, which comprises Dark Energy [1] and Dark Matter [2], remains unknown. That's a significant knowledge gap that has existed for a century. Consciousness [3], though not a fundamental of physics, is equally enigmatic. Its importance relies on the fact that scientific knowledge requires observation, and currently, we do not understand its role within the Cosmos. Despite these shortcomings, the two essential theories of QM [4] and GR [5] have vastly expanded our comprehension as descriptions of the extremely small (the standard model of particle physics [6]) and the macroscopically large (cosmic matter [7] and gravitational waves [8]). However, we have been unable to unite both theories through a solution for the quantization of gravity [9]. Though this may be a desired resolution, it would appear that such a unification may not exist. Perhaps there exists a single "theory of everything" [10] from which they both emerge and unite.

This is precisely what is proposed: a single integrative theory for dark energy, matter, and consciousness that succinctly provides a solution to their nature and can reproduce both the standard model of particle physics and the curved geometry of spacetime [11]. While current

leading models for dark matter, such as WIMPs [12] and axions [13] and dark energy like quintessence [14], provide significant insights, this work presents an alternative framework without relying on these specific mechanisms. The inclusion of a "Cosmic Observer"[15] within the model resolves several mysteries: A trigger for cosmogenesis [16], a purpose to the cosmos, a solution to the hard problem of consciousness [17], and the measurement problem [18] in QM, as well as a novel explanation for why matter exists as both animate and inanimate. The approach is a hypothesis that formulates a cosmogenesis in a non-relativistic space [19], in which the universe unfolds as a sequence of interactions between the Observer, Dark energy, and Dark matter. The model relies on observations from cold condensed matter physics [20], in which solitons [21], phonons [22], rotons [23], and vortex rings [24] serve as substrates for the emergence of a quantized particle-like energy field with geometric curvature. It also incorporates holography [25], generating holographic object and reference beams, which interfere on a lower two-dimensional boundary (the holographic plate), where time flows as shifting wave interferences [26, 27].

Over the last century, the Lambda-CDM (cold dark matter) model [28] has successfully explained the observable universe. The knowledge gained has not been discarded in the model's framing; for example, the (CMB) Cosmic Microwave Background [29], an accelerated expansion of the universe by dark energy [30], and the gravitational dark matter halos [31] creating galaxy and galaxy clusters are all retained. What is different is the establishment of the following: a cosmogenesis when none existed, a solution to the Hubble tension [32], the early appearances of (SMBH) supermassive black holes [33] and galaxies [34], an explanation for matter-antimatter asymmetry [35], the meaning of the fine structure constant [36], a new interpretation for

quantum entanglement [37] and the measurement problem, as well as a resolution to the hard problem of consciousness.

This paper's attempts at scientific inquiry rely on a conceptual, parsimonious model that satisfies Occam's razor [38, 39]. Karl Popper reflects this view in his quote, "Theories are nets cast to catch what we call 'the world': to rationalize, to explain, and to master it. We endeavor to make the mesh ever finer and finer." — Karl Popper, *The Logic of Scientific Discovery* (1959), p. 59. Einstein had a similar opinion, as reflected in his view, "The grand aim of all science is to cover the greatest number of empirical facts by logical deduction from the smallest possible number of hypotheses or axioms." — Albert Einstein, quoted in Philipp Frank's *Einstein: His Life and Times* (1947), p. 155. In acknowledging this tried and tested method of scientific inquiry and as a testament to the great minds, what is presented is a conceptual but highly plausible Integrative Theory of Dark Energy, Dark Matter, and Consciousness explaining the unexplained.

The Integrative Theory of Dark energy, Dark matter, and Consciousness

The Universe's cosmogenesis began in a non-relativistic higher dimension [40, 41] as a tightly coiled state of potential energy concealing within a dormant "Observer." Its energy stirred and unfolded into a geometric, vertical, bell-like structure, representing a steady-state solution that minimizes overall energy fluctuations, adhering to the principle of least action [42]. During this untangling, the Observer awakened in a state of pure observation [43, 44]. This new structure became a scalar field with linear symmetry [45, 46] displaying time and Lorentz invariances [47]. Noether's Theorem [48], developed by mathematician Emmy Noether, states that every

continuous symmetry of the action of a physical system corresponds to a conserved quantity. Therefore, if a scalar field's Lagrangian [49] density is time-invariant, as is the case here, the energy associated with that field is conserved. Following those principles, the field's evolution can be governed by a set of deterministic equations of motion derived from the Lagrangian, ensuring its behavior is consistent and predictable. This allows stable configurations (like solitons) to form without collapse or runaway expansion.

The stable, scalar energy field and the Observer's awakened presence triggered an excitement in its energy state, forcing a transition in the field's dynamics. This resulted in a torrent flow of kinetic energy exiting the field, propelling into a much higher plane as an entangled, convoluted stream of vivid, multicolored, multilayered lights. However, within this chaotic display was an order, for what was being illustrated from the point of view of the Observer were "geometric forms" drawn in brightly-colored light. This sequence of events broke the field's symmetry as it transitioned from linear to nonlinear. Its collapsed energy entered its lowest coherent ground state, having a temp of near absolute zero. Though not produced in the same manner as the Bose-Einstein Condensate (BEC) [50, 51], in condensed matter physics, many of the field's attributes and properties can be mirrored with BEC-like superfluidity [52]. In this model, it will be referenced as the Dark Matter [53] field of our Universe, which consists of a cosmic scalar field coupled to a macroscopic BEC waveform. After this transformation, the energy again flowed into the field as the entangled light fell from its excited state in one collective beam, merging with the field at its pinnacle ($E_{total}=E_{potential}+E_{kinetic}+E_{BEC)}$. This returning stream of kinetic energy becomes the Dark Energy of our Cosmos. Initial contact between the two resulted in a flurry of vibrational wave transmissions in two separate beams, pathways A and B. Within the perimeter of the bell-

shaped scalar field, pathway A flowed as a stream of soliton waves, having the properties of spin and orbital angular momentum [54] of varying frequency and amplitude. The flow gradient was from the field's peak to its lower two-dimensional boundary [55]. Pathway B, however, penetrated the BEC, becoming slowed in its downward trajectory. This resulted in two consequential outcomes for our observable universe—the first route, A, fashioned the inanimate physical matter of the universe, and the second route, B, gave rise to its living things (see Fig. 1).

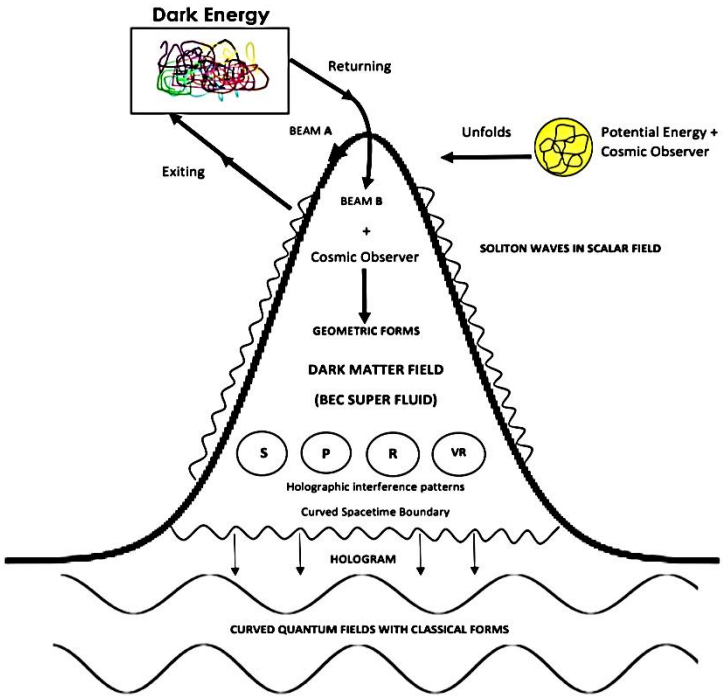

Fig. 1 Schematic Diagram of Cosmogenesis – (**S**) Soliton, (**P**) Phonon, (**R**) Roton, (**VR**) Vortex Ring

These phase transitions can be demonstrated in the language of mathematics. Commencing with the beam of pathway A, the following steps created our Cosmos.

1. The scalar field's ϕ linear symmetry can be represented in its static nature as a modified, non-relativistic, time-invariant Klein-Gordon equation [56] describing how the scalar field is distributed in space as:

$$\nabla^2\phi + \frac{dV(\phi)}{d\phi} = 0 \tag{1}$$

where; ∇^2 is the Laplacian operator representing its spatial derivatives. It specifically measures the curvature or the rate at which the scalar field spreads out in three-dimensional space. V (ϕ) is the potential energy function associated with the scalar field, $\frac{dV(\phi)}{d\phi}$ is the derivative of the potential energy for the scalar field ϕ indicating how its potential changes as the field varies. The Hamiltonian [57] describes the energy density, which sets the stage for its later kinetic energy dynamics as:

$$H_{\text{total}} = \int \left(\frac{1}{2}m|\nabla\phi|^2 + V(\phi)\right) d^3x \tag{2}$$

where; H_{total} is the total Hamiltonian of the scalar field ϕ, $\frac{1}{2}m|\nabla\phi|^2$ is the kinetic energy density of the field, and $V(\phi)$ is its potential energy density.

2. The Observer's presence within the field stimulates excitation, leading to kinetic energy exiting the system. The Lagrangian of the scalar field describes how its potential energy is converted to kinetic energy:

$$\mathcal{L} = \frac{1}{2}\left(\partial_\mu\phi\right)(\partial^\mu\phi) - V(\phi) \tag{3}$$

where; $(\partial_\mu \phi)(\partial^\mu \phi)$ is the kinetic term, $V(\phi)$ is the field's potential energy. The equation of motion derived from the Lagrangian is a modified Klein-Gordon-type equation shown as:

$$\partial_\mu \, \partial^\mu \phi + \frac{dV(\phi)}{d\phi} = 0 \tag{4}$$

This marks the transition from linear to nonlinear symmetry, leaving it in a Bose-Einstein Condensate (BEC)-like ground state. The Gross-Pitaevskii equation [58] represents the BEC wavefunction Ψ as:

$$\mu\Psi = -\frac{\hbar^2}{2M}\nabla^2\Psi + V_{\mathrm{BEC}}\Psi + g|\Psi|^2\Psi \tag{5}$$

where; μ is the chemical potential of the BEC Ψ , $-\frac{\hbar^2}{2M}\nabla^2\Psi$ is the kinetic energy of the condensate, $V_{\mathrm{BEC}}\Psi$ represents the external trapping potential acting on the condensate, g is the coupling constant for the BEC interactions.

The energy E of the scalar field ϕ can be represented by a non-relativistic version of the Schrodinger equation given by:

$$-\frac{\hbar^2}{2m}\nabla^2\phi + V(\phi)\phi = E\phi \tag{6}$$

The Hamiltonian H for the system holistically describes it as a static energy field:

$$H = \int \left(\frac{\hbar^2}{2m}|\nabla\phi|^2 + V(\phi)|\phi|^2 + g|\Psi|^4 + \lambda|\Psi|^2|\phi|^2\right) d^3x \tag{7}$$

where; $\frac{\hbar^2}{2m}|\nabla\phi|^2$ represents the kinetic energy of the scalar field ϕ , m is its mass and $\nabla\phi$ is its spatial gradient, $V(\phi)|\phi|^2$ represents its potential energy, $g|\Psi|^4$ is the self-interaction for the BEC field Ψ , $\lambda|\Psi|^2|\phi|^2$ represents the interaction energy between the fields with λ as the coupling constant.

3. The kinetic (Dark) energy that exited the field falls back down, returning to interact with the peak of the scalar field, generating solitons that propagate along its peripheral boundary as:

$$E_{\text{kinetic}}\,(r,\theta) = \beta\cos\,(\omega r)\sin\,(m\theta) \tag{8}$$

where; $\cos\,(\omega r)$ captures the oscillatory wave-like behavior of the kinetic energy, r is the radial distance from its origin, $\sin\,(m\theta)$ represents angular motion, m is a quantum number (similar to the orbital quantum number in atomic systems), β is the amplitude of the kinetic energy modulating both oscillations and angular motion.

Solitons are localized, stable energy packets that do not change their shape or velocity while propagating. The soliton solutions are described by:

$$\phi(x,t) = A\text{sech}\,\left(\frac{x-vt}{\Delta}\right)e^{i(kx-\omega t)} \tag{9}$$

where; A is the amplitude, v is the velocity of the soliton, Δ is the width, k and ω are the wave number and frequency, respectively, of the solitons.

Solitons are modeled as excitations within the scalar field, similar to electrons within the Quantum Field Theory's (QFT) fermion field [59]. They are coupled to the scalar field as follows:

$$\mu\psi = \left(-\frac{\hbar^2}{2m}\nabla^2 + g\phi\right)\psi \tag{10}$$

where; μ is the chemical potential of the soliton, ψ is the soliton, m is the mass of the soliton, ∇^2 is the Laplacian operator representing the spatial distribution of the soliton, $g\phi$ is the coupling strength between the soliton and scalar fields.

They also possess ½ integer spin and orbital angular momentum given as:

$$\Psi(\mathbf{r},t) = \Phi(r)e^{i(m\theta+kz-\omega t)} \tag{11}$$

where; $\Psi(\mathbf{r},t)$ is the soliton field, $\Phi(r)$ is the radius of the soliton, $m\theta$ is the angular phase, kz is its longitudinal wave vector, describing soliton movement along the z-axis, ωt is the frequency associated with the soliton's energy.

The soliton is modeled to have a two-component spinor field; $\psi(x) = \binom{\psi_1(x)}{\psi_2(x)}$, $\psi_1(x)$ spin up and $\psi_2(x)$ spin down. Anti-commutation relations on the spinor field $\psi(x)$, ensures no violation of the Pauli exclusion principle [60]; $\{\psi_i(x), \psi_j(y)\} = \psi_i(x)\psi_j(y) + \psi_j(y)\psi_i(x) = 0$ for all $x \neq y$ and for all components i, j , where *i*, *j*=1,2 correspond to the two components of the spinor field (spin-up and spin-down). For solitons at the same point in space:

$$\psi_i(x)\psi_i(x) = 0 \tag{12}$$

The Pauli equation [61] describes the dynamics of the soliton in a non-relativistic framework. This equation governs how the soliton moves through space, interacts with the scalar field's potential, and how its spin interacts with external fields:

$$i\hbar\frac{\partial\psi}{\partial t} = \left[-\frac{\hbar^2}{2m}\nabla^2 + V(\mathbf{r}) - \frac{e\hbar}{2m}\boldsymbol{\sigma}\cdot\mathbf{B}\right]\psi \tag{13}$$

where; ψ is the two-component spinor field representing the soliton, **σ** are the Pauli matrices [62] representing the spin operators $(\sigma_x, \sigma_y, \sigma_z), \sigma_x = \begin{pmatrix}0 & 1\\ 1 & 0\end{pmatrix}, \sigma_y = \begin{pmatrix}0 & -i\\ i & 0\end{pmatrix}, \sigma_z = \begin{pmatrix}1 & 0\\ 0 & -1\end{pmatrix}$, $V(\mathrm{r})$ is the potential energy landscape of the scalar field, **B** is the magnetic field interacting with the soliton's spin, and m is the mass of the soliton.

The Lagrangian equation governs the overall dynamics of the system; $V(\phi)$ is the potential energy of the scalar field. It captures the interaction between the soliton's spinor and the scalar field as:

$$\mathcal{L} = \bar{\psi}\left(i\gamma^{\mu}\,\partial_{\mu} - m\right)\psi + \frac{1}{2}\left(\partial_{\mu}\phi\right)^{2} - V(\phi) \tag{14}$$

where; $\bar{\psi} = \psi^{\dagger}\gamma^{0}$ is the Dirac adjoint two-component spinor field ψ , $\gamma\mu$ are the Dirac matrices (which are reduced to Pauli matrices in our non-relativistic case), m is the mass of the soliton, $\frac{1}{2}\left(\partial_{\mu}\phi\right)^{2}$ is the kinetic term for the scalar field ϕ .

The soliton frequency generated by the different energy inflows directly influences its properties. Its mass is related to the amplitude A and frequency ω of its oscillation. The energy contained in the soliton is given by: $E_{\text{soliton}} = \hbar\omega$, where $\hbar$ is the reduced Planck constant [63]. The amplitude of the soliton reflects the energy density localized in the soliton, and thus, its contribution to the total mass is given as:

$$m_{s} = \frac{E_{\text{soliton}}}{c^{2}} = \frac{\hbar\omega}{c^{2}} \tag{15}$$

where m_{s} is the mass of soliton in its lowest ground state. A larger amplitude would imply more localized energy in the soliton ($E_{\text{soliton}} \propto A^{2}$), resulting in a heavier "particle" mass to its nature when quantized. The theory allows for solitons of higher energies to exist in quantized forms as Muon and Tau electrons [64], which are heavier and have greater energy densities:

$$m_{\mu} = \frac{\hbar\omega_{\mu}}{c^{2}}, m_{\tau} = \frac{\hbar\omega_{\tau}}{c^{2}} \tag{16}$$

where; m_{μ} is the mass of muon, m_{τ} is the mass of tau.

A tau electron (a high-frequency soliton) could lose energy through interactions with the scalar field, eventually decaying into a muon or an electron (lower-frequency solitons), depending on the dynamics of the interaction. These can exit the scalar field as high-energy cosmic waves (muons/tau). There might also be new lepton-like states (potentially higher than the tau) at even higher frequencies, which could be discovered in high-energy particle physics experiments. The feedback loop maintains energy conservation through the oscillatory decay of kinetic energy: $E_{\text{total}} = E_{\text{kinetic}}(t) + E_{\text{muons / tau particles}}(t)$

The interaction between the scalar field ϕ and the BEC Ψ can generate high-energy exchanges, facilitating feedback loops. Solitons' angular momentum or spin-related properties could lead to fermionic behavior once they interact with the BEC. The Hamiltonian captures the entanglement between the fields:

$$H_{\text{entanglement}} = \int (\alpha \phi^{\dagger}\Psi + \beta(\nabla\phi)^{\dagger}(\nabla\Psi))d^3x \quad (17)$$

where; α and β represent the coupling constants that control the strength of the entanglement, $\phi^{\dagger}\Psi$ represents the entanglement, $(\nabla\phi)^{\dagger}(\nabla\Psi)$ couples their gradients and models their cyclic or oscillatory interactions over space. The cyclical energy transfer between the scalar field and BEC can be shown as: $\frac{dE_{\text{scalar}}}{dt} = -\frac{dE_{\text{BEC}}}{dt} = f(\phi, \Psi)$, ensuring energy is conserved but constantly oscillating between the two fields.

4. **Black Holes, EM field, protons, neutrons, strong and weak forces.**

The initial contact from the returning dark energy generates density perturbations [65] within the BEC superfluid, patterned similarly to its entangled higher-dimensional form, creating a cosmic-like web [66]. This becomes a blueprint for how all excitations within the BEC superfluid Ψ are gathered and disseminated as shown by:

$$\mu\delta\Psi = \left(-\frac{\hbar^2}{2m}\nabla^2\delta\Psi + g|\Psi_0|^2\delta\Psi + \lambda\Phi\Psi_0\right) \quad (18)$$

The perturbations $\delta\Psi$ describe the spatial variations in the density of the BEC superfluid induced by the interaction with the dark energy field Φ, μ is the chemical potential, g is the self-interaction strength of the BEC, $\lambda\Phi$ represents the coupling between the dark energy and the BEC superfluid. The density perturbation δ can be written as: $\nabla^2\delta = \frac{\lambda}{\hbar^2}\Phi\Psi_0$, where δ represents the density contrast in the BEC and $\Phi\Psi_0$ is the source term that drives the perturbations with Ψ_0 being the unperturbed wave function of the BEC. This equation shows how the spatial structure of the dark energy influences the density perturbations in the BEC**.**

Solitons entering the BEC transfer their angular momentum into the superfluid, producing oscillatory and rotational effects and transforming into dark and bright solitons [67]. In a BEC, a dark soliton is a region where the density drops to near zero, representing a topological defect or localized disturbance. Dark solitons are stable and can move through the condensate while maintaining their structure, similar to how black holes [68] persist in spacetime. Bright solitons have their energy densities amplified and can be analogous to stars [69] as localized, stable energy concentrations. Solitons can become trapped within the vortex core, forming soliton bubbles [70]. These modes produce pressure waves, which collapse into other collective excitations as phonons and the higher momentum roton and vortex rings. Phonons are analogous

to sound or acoustic waves, having very long wavelengths, and can couple to other phonons as they propagate through the system. Inelastic interactions can give rise to soliton trains [71], comparable to the galactic string of pearls [72] in astronomy. These modes can be modeled using a modified Gross-Pitaevskii equation for a BEC ψ with added terms to account for angular momentum as:

$$i\hbar \frac{\partial \psi}{\partial t} = \left[-\frac{\hbar^2}{2m}\nabla^2 + V_{\text{ext}} + g|\psi|^2 - \frac{\hbar^2 m^2}{2mr^2} \right] \psi \tag{19}$$

where; $\frac{\hbar^2 m^2}{2mr^2}$ is a centrifugal potential to account for the angular momentum, V_{ext} is the external potential, $g|\psi|^2$ is a nonlinear interaction term, $-\frac{\hbar^2}{2m}\nabla^2$ is a kinetic energy operator.

The coupling Hamiltonian for solitons ϕ and phonons Ψ interactions can be written as:

$$H_{\text{interaction}} = \int (\lambda_1 |\phi|^2 |\Psi|^2 + \lambda_2 |\nabla\phi|^2 |\nabla\Psi|^2 + \lambda_3 \mathbf{J}^2) d^3x + \lambda_4 \mathbf{J} \cdot (\nabla \times \mathbf{v}) \tag{20}$$

where; $\lambda_1, \lambda_2, \lambda_3$ are coupling constants, **J** represents the angular momentum density of solitons, λ_4 is a coupling constant for rotational interactions between soliton and phonon, $|\nabla\phi|^2$ and $|\nabla\Psi|^2$ are momentum coupling, $|\phi|^2$ is the density of the solitons, $|\Psi|^2$ is the density of the phonons.

4.1 **Black hole formation**.

Soliton behavior in a BEC can serve as an analogy to phenomena in the universe, including black holes and other cosmological phenomena. In particular, vortex rings and vortices in a BEC can exhibit dynamics similar to rotating black holes (Kerr black holes [73]). A vortex in a BEC has a central region of low or zero density (identical to the event horizon of a black hole) surrounded

by a circulating superfluid. This circulating motion can be considered analogous to the frame-dragging [74] near a rotating black hole. Dark soliton collisions in a BEC often result in the transfer or redistribution of energy, which can be analogous to the gravitational wave emission that occurs during black hole mergers. Dark solitons can exhibit properties like phase shifts and energy localization, which are somewhat analogous to the event horizon of a black hole, where specific physical effects (like the inability of matter or light to escape) can occur. However, dark solitons as a model for black hole generation may not have a singularity [75] at their core.

As collapsed structures, dark solitons would naturally collect in areas where the density perturbations are at their greatest, forming larger dark soliton pools. These gravitational patterns could explain the early presence of SMBHs at nearly every galaxy's center. They can also serve as the initial cosmic seeds for the dark matter halos, guiding the formation of galaxies and galaxy clusters [76].

A dark soliton wavefunction can be modeled as:

$$\Psi(x,t) = \Psi_0 \left[i\sin(\theta) + \cos(\theta)\tanh\left(\frac{x-vt}{\xi}\right)\right] e^{-i\mu t/\hbar} \tag{21}$$

where; Ψ_0 is the background condensate density, v velocity of the soliton, $\xi = \frac{\hbar}{\sqrt{2mgn}}$ is the healing length (the characteristic length scale of the soliton), θ is the phase shift across the soliton, μ is the chemical potential of the BEC. This solitonic structure could be analogous to a black hole, where the tanh term represents a sharp density contrast akin to the event horizon.

4.2 **The Electromagnetic Field, Force, and the Fine Structure Constant.**

Soliton bubbles within a BEC superfluid medium have been observed to form soliton pairs, described as Cooper pairs [77]. They can do this by coupling to a phonon, which assumes the role of energy exchanger. The soliton integers in the pair can cancel each other, producing a boson of 0 or 1 integer. Solitons can generate electrical and magnetic fields in condensate states. Their respective wavefunctions overlap into one wavefunction (U1 symmetry of Quantum Electrodynamics [78]; QED). This interaction creates an effective electromagnetic interface between the solitons, generating an electromagnetic field. The Hamiltonian for this soliton-phonon coupling can be written as:

$$H_{\text{soliton-phonon}} = g\int (|\phi_1(\mathbf{r},t)|^2 + |\phi_2(\mathbf{r},t)|^2)\left|\Psi_{\text{phonon}}(\mathbf{r},t)\right|^2 d^3x \tag{22}$$

where; $\phi_1(\mathbf{r},t)$ and $\phi_2(\mathbf{r},t)$ represent the two soliton(quasiparticles [79]) fields, $\Psi_{\text{phonon}}(\mathbf{r},t)$ phonon field, g is the coupling constant**.**

The phonon field transfers energy between the two solitons in a periodic or oscillatory fashion. This can be modeled as follows:

$$H_{\text{cyclic}} = \int \left(\lambda_1\phi_1^\dagger\nabla\Psi_{\text{phonon}} + \lambda_2\phi_2^\dagger\nabla\Psi_{\text{phonon}}\right)d^3x \tag{23}$$

where; λ_1 and λ_2 are constants that control the strength of the energy exchange between each soliton and the phonon field. The gradient term $\nabla\Psi_{\text{phonon}}$ indicates that changes in the phonon field mediate the energy exchange. The phonon's rotational dynamics could give it the necessary angular momentum to behave like a spin-1 boson and become the electromagnetic force.

$$\mathcal{L}_{\text{Higgss-phonon}} = g_H|\phi_H|^2\left|\Psi_{\text{phonon}}\right|^2 = 0 \tag{24}$$

where; ϕ_H is a Higgs field, Ψ_{phonon} is the phonon field, and g_H is a coupling constant, which shows that there are zero interactions.

4.2.1 **The fine structure constant.**

The fine structure constant α is a dimensionless constant that characterizes the strength of the electromagnetic interaction between charged particles, such as electrons and protons, given as:

$$\alpha = \frac{e^2}{4\pi\epsilon_0 \hbar c} \approx \frac{1}{137} \tag{25}$$

The following is a possible solution to the mystery of $\frac{1}{137}$. The model's electromagnetic field (EM) comprises two solitons (electrons when quantized) exchanging energy with a phonon (photon) as the electromagnetic force carrier. However, the soliton-soliton interaction behaves as a Coulomb-like electrostatic potential in the model.

The electrostatic potential energy U between the two solitons due to their electromagnetic interaction can be described as: $U_{\text{soliton-soliton}} = \frac{e^2}{r}$, where r is the distance between the solitons and e^2 represents the effective charge of each soliton. The energy exchanged between solitons via the phonon is given as: $E_{\text{exchange}} = \hbar\omega_{\text{phonon}}$

$$\alpha = \frac{U_{\text{soliton-soliton}}}{E_{\text{exchange}}} = \frac{\frac{e^2}{r}}{\hbar\omega_{\text{phonon}}} \tag{26}$$

For this to be dimensionless, ω_{phonon} has to be expressed in a way that cancels the units of length r. Let's express ω_{phonon} in terms of the speed of light and the distance between solitons as:

$$\omega_{\text{phonon}} \sim \frac{c}{r} \qquad \alpha = \frac{\frac{e^2}{r}}{\hbar\frac{c}{r}} = \frac{e^2}{\hbar c} \tag{27}$$

This result matches the traditional form of the fine structure constant α, which can be seen as the ratio between the strength of the electromagnetic force and the speed of light (which sets the scale for the electromagnetic interaction in relativistic systems).

The EM field thus consists of three structure waves corresponding to the two solitons (A_1A_2) and the phonon (A_3) shown as:

$$\alpha = \frac{e^2}{\hbar c} \sim \frac{U_{\text{soliton-soliton}}}{E_{\text{exchange}}} = \frac{A_1A_2}{A_3} \tag{28}$$

This equation expresses the fine structure constant as a ratio of the amplitudes of the soliton-phonon interactions, which describes how the electron's orbital field is built from these structure waves. If we assume that α is known (approximately as $\frac{1}{137}$, we can solve for the relationship between the amplitudes of the soliton and phonon waves: $A_1A_2 = \alpha A_3$

$$A_1A_2 = \frac{1}{137}A_3 \tag{29}$$

If we assume that the amplitudes of the soliton waves are equal, meaning that both A_1 and A_2 contribute equally to the interaction, the equation (29) can be simplified by letting:

$$A_1 = A_2 = A_{\text{soliton}} \quad \text{then} \quad A^2_{\text{soliton}} = \frac{1}{137}A_3 \quad \text{and} \quad A_3 = 137A^2_{\text{soliton}} \tag{30}$$

Hence, each soliton's interaction contributes to the overall wave structure of the EM field. This can be written as:

$$\Psi_{\text{orbital}}(r, \theta, t) = \sum_{n=1}^{3} A_n \cos(k_n r - \omega_n t + \phi_n) \tag{31}$$

where; A_n are the amplitudes of the fine structure waves, k_n are the wave numbers for the solitons and phonon, ω_n are the angular frequencies for the solitons and phonon, ϕ_n are the phase shifts for each wave component (soliton or phonon). This explains why the fine structure appears in the Lyman-alpha lines of hydrogen [80].

The fine structure constant can also be defined by the relationship between the electron's charge and the speed of light. A photon must supply enough energy to overcome the binding energies E_{binding} of the soliton (Cooper) pair, which can be written as:

$$E_{\text{photon}} \geq E_{\text{binding}} = 2m_e c^2 - \Delta E_{\text{binding}} \tag{32}$$

When a photon breaks the Cooper pair, the electrons are ejected, and their kinetic energy is given by: $E_{\text{kinetic}} = E_{\text{photon}} - E_{\text{binding}}$

The velocity of the electron v_e is related to its kinetic energy: $E_{\text{kinetic}} = \frac{1}{2} m_e v_e^2$, where

$$v_e = \sqrt{\frac{2E_{\text{kinetic}}}{m_e}} \tag{33}$$

Therefore, the electron's velocity v_e after photoemission is related to the photon's energy and its interaction with the electromagnetic field as governed by the fine structure α:

$$\alpha = \frac{e^2}{\hbar c} \qquad \alpha \propto \frac{e^2}{v_e} \tag{34}$$

This expression shows that the fine structure constant is related to the electron's charge and velocity after breaking the Cooper pair. This correctly predicts the fine structure constant by modeling the interaction between soliton-like electrons and phonons.

4.3 **Protons, Neutrons, and the Strong force**.

Soliton interactions in a superfluid BEC can be modeled as exhibiting fermionic behavior as described by the Standard Model of Particle Physics. Soliton-soliton and soliton-phonon-roton dynamics can generate new collective excitations that give rise to fermionic quasiparticles. Depending on the strength and nature of the phonon coupling, the soliton could split into multiple quasiparticles, each carrying a fraction of the original soliton's charge. This is analogous to fractional quantum Hall states [81], where collective excitations can have fractional charges $\left(\frac{e}{3}, \frac{e}{5}\right)$ and serve as analogs to up and down quarks; Up quark: Charge = $+\frac{2}{3}$, Down quark: Charge =$-\frac{1}{3}$. Suppose the soliton has a charge of −1 (as an electron analog), and the phonon gains a charge of $+\frac{5}{3}$ through energy transfer, the combined system (up quark-quasiparticle) would have a net charge of: $-1+\frac{5}{3}=+\frac{2}{3}$. A soliton-phonon pair could create a down quark if the soliton's charge is -1 and the phonon carries a fractional charge of $+\frac{2}{3}$; the net charge for the soliton-phonon pair would be: $-1+\frac{2}{3}=-\frac{1}{3}$

The coupling between a soliton of frequency ω_1 and a phonon in the BEC could produce a quark field:

$$H_{\text{interaction}} = \lambda_1 \phi(\omega_1)\Psi \tag{35}$$

where; $\phi(\omega_1)$ represents a soliton with frequency ω_1 and Ψ is the BEC phonon field.

A proton [82] consists of two up and one down quark (uud). The phonon interaction results in a proton with a net charge of +1. A neutron [83] consists of one up quark and two down quarks (udd). The phonon interaction leads to the formation of a neutron with a net charge of 0.

Vortex cores [84] can act as potential wells in a superfluid, trapping quasiparticles inside. The confinement [85] of quarks inside hadrons (protons and neutrons) can be compared to the vortex's trapping of quasiparticles.

The Gross-Pitaevskii equation (GPE) describes the dynamics of the superfluid BEC. For vortex formation and the trapping of quasiparticles, the GPE can be modified as follows:

$$i\hbar \frac{\partial \Psi(\mathbf{r},t)}{\partial t} = \left(-\frac{\hbar^2}{2m}\nabla^2 + V_{\text{ext}}(\mathbf{r}) + g|\Psi(\mathbf{r},t)|^2 + V_{\text{vortex}}(\mathbf{r})\right)\Psi(\mathbf{r},t) \quad (36)$$

where; $\Psi(\mathbf{r},t)$ is the condensate wavefunction, $\mathbf{r}$ is a point in space and t specifies the moment at which the wave function Ψ is evaluated, $g|\Psi(\mathbf{r},t)|^2$ is the interaction that generates the quasiparticle excitations. The vortex potential $V_{\text{vortex}}(\mathbf{r})$ can be represented as: $V_{\text{vortex}}(\mathbf{r}) = \frac{mv_{\text{vortex}}^2}{2}$ where v_{vortex} is the velocity of the fluid around the core.

The quasiparticles representing "quarks" can be modeled as localized excitations within the vortex, $\Phi(\mathbf{r},t)$ describes the quark wavefunction trapped in the vortex as:

$$i\hbar \frac{\partial \Phi(\mathbf{r},t)}{\partial t} = \left(-\frac{\hbar^2}{2m}\nabla^2 + V_{\text{trap}}(\mathbf{r})\right)\Phi(\mathbf{r},t) \quad (37)$$

Protons and neutrons are the composite states formed when three quasiparticles are confined within a vortex core. A three-body potential [86] is used to describe the interaction between the quasiparticles (quarks) inside the vortex core as:

$$V_{\text{three-body}} = \lambda_3 \sum_{i<j} \left|\Phi_i - \Phi_j\right|^2 \quad (38)$$

where; λ_3 is the strength of the interactions between the quarks, Φ_i is the wave function of the quarks trapped within the vortex core. $V_{\text{three-body}}$ describes the interaction between the quasiparticles (quarks) to form protons and neutrons.

The strong nuclear force [87] could be modeled through the energy exchange between solitons via the quark field's phonons. This phonon field can be thought of as a gluon-like field [88], which can be modeled by the interaction Lagrangian as:

$$\mathcal{L}_{\text{int}} = -\frac{1}{4}F^a_{\mu\nu}F^{\mu\nu}_a + g_s\bar{\psi}\gamma^\mu A^a_\mu T_a\psi \tag{39}$$

where; $F^a_{\mu\nu}$ is the field strength tensor of the gluon-like field, g_s is the coupling constant, A^a_μ is the gauge field generated from the soliton-phonon interactions, acting as the gluon**,** T_a is the generators of the SU(3) symmetry group, akin to Quantum Chromodynamics; QCD, $\bar{\psi} = \psi^\dagger\gamma^0$ is the Dirac adjoint of the fermion field, γ^μ are the gamma matrices describing the spin structure of the fermions.

The field strength tensor for the gluon-like field would involve the soliton frequencies ω_i and the energy exchange between the solitons and phonons. We can write the effective gauge field equations as:

$$F^a_{\mu\nu} = \partial_\mu A^a_\nu(\omega_i) - \partial_\nu A^a_\mu(\omega_i) + g_s f^{abc}A^b_\mu(\omega_i)A^c_\nu(\omega_i) \tag{40}$$

where $A^a_\mu(\omega_i)$ is the gluon-like field generated by solitons of frequency ω_i .

The concept of color confinement in QCD [89] (where quarks are bound within protons and neutrons by gluons) can be mirrored by the vortex confinement of quasiparticles in the BEC**.**

The energy *E* of a vortex ring in a superfluid can be described as:

$$E_{\text{vortex}} \propto \rho_s \kappa^2 R \ln\left(\frac{R}{a_0}\right) \tag{41}$$

where; ρ_s is the superfluid density, κ is the circulation quantum (related to the angular momentum), R is the radius of the vortex ring, a_0 is the core size of the vortex.

Vortex rings [90] can create regions of localized energy and angular momentum within the superfluid. If quarks are housed within this potential, the coupling between quasi-soliton and phonons could be responsible for generating the binding energy [91]. This binding energy would then contribute to the mass of the proton or neutron, as the energy trapped in the vortex ring would translate into mass via $E = mc^2$. The vortex ring could serve as the confinement mechanism for quarks, giving rise to the different quark flavors and a hierarchy of the mass energies of the strange, bottom, charm, and top quarks described by QCD. The vortex ring confines the influence of the Gluon's strong force. One can imagine the quasi-solitons coupled to the phonon (gluon) being tugged and rotated within the vortex.

The energy of the quark-like system trapped in the vortex ring can be expressed as:

$$E_{\text{binding}} = \lambda_{\text{coupling}}\, \rho_s \kappa^2 R \ln\left(\frac{R}{a_0}\right) \tag{42}$$

The total mass of a composite particle like a proton or neutron is the sum of the intrinsic energy of the quarks and the binding energy from the quasi-soliton-phonon interactions within the vortex ring:

$$m_{\text{proton}} = \sum_{\text{quarks}} \frac{\hbar \omega_{\text{quark}}}{c^2} + \frac{E_{\text{binding}}}{c^2} \tag{43}$$

4.4 **The weak force.**

Rotons can affect the energy exchange between solitons and phonons, influencing quasiparticle formation**.** Roton-phonon interactions might lead to quasiparticle (quasi-solitons) transitions that mimic the behavior of flavor-changing weak interactions. The massive rotons would interact weakly, only mediating short-range interactions in the superfluid, much like W and Z bosons in the weak force. Rotons could be responsible for the electroweak unification of the U(1) x SU(2) symmetry in QED. When the symmetry is broken, rotons behave like W and Z bosons.

The Hamiltonian describing the three-body bound state in the vortex trap, including phonon and roton contributions, would be as follows:

$$H_{\text{total}} = H_{\text{soliton}} + H_{\text{soliton-phonon}} + H_{\text{roton}} + V_{\text{3-body}}(\mathbf{r}_1, \mathbf{r}_2, \mathbf{r}_3)$$

$$H_{\text{roton-phonon-soliton}} = g_T \int |\Psi_{\text{roton}}|^2 \left|\Psi_{\text{phonon}}\right|^2 |\phi_{\text{soliton}}|^2 d^3x$$

$$H_{\text{roton mass}} = \frac{m_{\text{roton}}^2}{2} \int |\Psi_{\text{roton}}|^2 d^3x$$

$$H_{\text{roton-soliton}} = g_{\text{weak}} \int (|\phi_{\text{soliton}}|^2 |\Psi_{\text{roton}}|^2) d^3x \tag{44}$$

where; g_T is the roton-assisted coupling constant, which determines how strongly the roton affects the phonon-soliton interaction. The roton-soliton interaction Hamiltonian could take the form g_{weak} as the weak coupling constant for roton-soliton interactions.

Roton coupling could induce a similar decay process, where the configuration of quasi-solitons (quarks) changes, leading to proton-like or neutron-like decay shown by:

$$H_{\text{decay}} = \int \left(g_w \Psi_{\text{roton}} \left(\phi_u^\dagger \phi_d\right) + g'_w \Psi_{\text{roton}} \left(\phi_d^\dagger \phi_u\right) \right) d^3x \tag{45}$$

where; g_w and g'_w represent the coupling constants for the weak decay interactions mediated by the roton (analogous to the W and Z bosons). Essentially, a roton acts as a cyclic energy exchange medium coupling a neutron and proton waveform, similar to the Lie group SU(2) symmetry. In this manner, a neutron can transition into a proton and vice versa.

The boson fields (such as W and Z bosons) mediate the interactions between solitons (quark-like excitations) in the BEC. The boson fields can be introduced via gauge invariance by the Lagrangian:

$$\mathcal{L}_{\text{boson}} = -\frac{1}{4}F^a_{\mu\nu}F_a^{\mu\nu} + \bar{\Psi}\gamma^\mu\left(D_\mu - m\right)\Psi \tag{46}$$

where; $F^a_{\mu\nu}$ represents the field strength tensor of the boson fields, a is an index for the gauge fields (like $W^\pm$ and Z^0 bosons), D_μ is the covariant derivative associated with the boson fields, $\bar{\Psi}\gamma^\mu$ represents the interaction between the fermions (solitons) and the gauge bosons, and m is the mass term, $-\frac{1}{4}F^a_{\mu\nu}F_a^{\mu\nu}$ describes the self-interactions and dynamics of the bosons (like W and Z bosons) through the field strength tensor, $\bar{\Psi}\gamma^\mu\left(D_\mu - m\right)\Psi$ represents the interaction between the solitons (quarks) and the boson fields (gauge fields).

5. **The Higgs field, Boson, and Fermion mass.**

The cyclic energy exchange between the scalar field and the BEC could generate a Higgs scalar field ϕ [92]. The potential energy of the soliton-BEC system can model the Higgs-like field [93], which can be written as:

$$V_{\text{Higgs}}(\phi) = \frac{\mu^2}{2}\phi^2 - \frac{\lambda}{4}\phi^4 \tag{47}$$

where; μ^2 represents the mass scale associated with the Higgs field ϕ, λ controls its self-interaction, allowing it to acquire a non-zero vacuum expectation value (VEV) [94] for spontaneous symmetry breaking [95]. The (VEV) represents the point where the potential reaches its minimum.

If ($\mu^2 < 0$), the field's potential looks like a Mexican hat [96] (a circular valley). It will "settle" at some point along the bottom of the valley rather than staying at the peak, breaking the symmetry. The Higgs field "chooses" a value that is not zero everywhere in space.

Before symmetry breaking, the Higgs field sits at $\phi = 0$, and the system is symmetric. An increase in temperature generated from stress-energy-momentum tensors [97] within the BEC (Higgs-like) field can decouple the energy exchanges between solitons, phonons, and rotons leading to symmetry breaking. This has been observed as the breaking of cooper pairs as temperature increases in superconductor mediums. Once the Higgs field acquires its non-zero vacuum expectation value (VEV), symmetry is broken. The value of the field becomes $\phi = v \neq 0$ The Higgs field emerges following a Yukawa [98] interaction [99] shown by the Lagrangian as:

$$\mathcal{L}_{\text{Higgs}} = -g_{\text{Yukawa}}\,\phi\Psi\overline{\Psi} \tag{48}$$

where; g_{Yukawa} is the coupling constant between the Higgs field ϕ and the fermion field Ψ (which represents quarks and leptons), $\overline{\Psi} = \Psi^{\dagger}\gamma^0$ is the Dirac adjoint of the fermion field, $\overline{\Psi}\Psi$ represents the mass of the fermion after interacting with the Higgs field.

When the Higgs field acquires its non-zero VEV, the soliton (electron-fermion) field effectively "feels" this VEV everywhere in space. This interaction leads to the mass of the electron; m_e being determined by the strength of the Higgs-electron coupling (g_{Yukawa}), and the Higgs field's VEV $\langle\Psi\rangle$:

$$m_e = g_{\text{Yukawa}} \langle\Psi\rangle \tag{49}$$

Heavier versions of the electron arise from stronger Yukawa interactions with the Higgs-like field:

$$\mathcal{L}_{\text{Yukawa}} = -g^f_{\text{Yukawa}} \phi_f \Psi$$

$$m_e = g^e_{\text{Yukawa}} \langle\Psi\rangle, m_\mu = g^\mu_{\text{Yukawa}} \langle\Psi\rangle, m_\tau = g^\tau_{\text{Yukawa}} \langle\Psi\rangle$$

$$g^\tau_{\text{Yukawa}} > g^\mu_{\text{Yukawa}} > g^e_{\text{Yukawa}} \tag{50}$$

where; ϕ_f is the soliton field representing either the electron e , muon μ, or tau τ, and g^f_{Yukawa} is the coupling strength, which increases for the heavier particles and $\langle\Psi\rangle$ represents the Higgs-like field's VEV**.**

The emergence of the electroweak, strong force components and Higgs Boson [100] can be described as an interaction framework where the Higgs field Φ_{Higgs} is connected to the soliton, quark, and gauge fields as:

$$\Phi_{\text{Higgs}} = \lambda_{\text{soliton}} |\phi_{\text{soliton}}|^2 + \lambda_{\text{quark}} \left|\phi_{\text{quark}}\right|^2 + \frac{1}{2} g_{\text{EW}} W_\mu W^\mu + \frac{1}{2} g_{\text{strong}} G^{\mu\nu}_a G^a_{\mu\nu} \tag{51}$$

where; $\frac{1}{2} g_{\text{EW}} W_\mu W^\mu$ represents the electroweak interaction, W_μ is the field strength tensor for the W boson, g_{EW} is the electroweak coupling constant, $G^{\mu\nu}_a$ is the field strength tensor for the

gluon field (strong interaction), $\lambda_{\text{soliton}} |\phi_{\text{soliton}}|^2$ is the interaction between the Higgs field and the soliton field, $\lambda_{\text{quark}} |\phi_{\text{quark}}|^2$ is the Higgs interaction with the quark field.

The Higgs boson arises from the interaction between the scalar field and the BEC or boson fields. Since the scalar field and BEC are chosen to contribute without introducing charge or spin, the resulting Higgs boson is a scalar particle (spin-0) and neutral (no charge). The Higgs boson emerges as a bound state of various interacting fields, including solitons (fermions such as quarks, electrons, muons, and tau leptons) and boson fields (representing the electroweak and strong forces).

This equation describes the mass of the Higgs boson as the second derivative of the potential; $V(\phi_{\text{scalar}}, \Psi_{\text{BEC}})$ with respect to the scalar field ϕ_{scalar} , evaluated at the vacuum expectation value $(\text{VEV})\phi = v$ shown as:

$$m_{\text{Higgs}}^2 = \frac{\partial^2 V(\phi_{\text{scalar}}, \Psi_{\text{BEC}})}{\partial \phi_{\text{scalar}}^2}\bigg|_{\phi=v} \tag{52}$$

It shows how the Higgs boson mass arises from the curvature of the potential, which includes contributions from the scalar field, BEC, or boson fields and their interactions. The second derivative of the potential determines how steep the potential is at its minimum (the vacuum expectation value), which determines the Higgs boson's mass.

In a superfluid BEC, excitations (like solitons or vortex rings) can be confined or trapped, preventing their energy from fully interacting with other fields. The superfluidity can cause screening [101] by allowing specific excitations to move through the BEC without dissipating energy, meaning that not all the available energy is transferred to the Higgs boson. This reduction

in energy transfer could limit how much mass the Higgs boson gains, keeping it lighter than expected.

5.1 **Mass of protons and neutrons.**

The quarks themselves get their small masses via the Higgs mechanism. For example:

Up quark mass: $m_u \approx 2.2\mathrm{MeV/c^2}$ Down quark mass $m_d \approx 4.7\mathrm{MeV/c^2}$

However, the sum of the quark masses is much smaller than the total mass of the proton or neutron, about $940\mathrm{MeV/c^2}$. The mass of protons and neutrons comes from the binding energy between solitons mediated by phonon interactions, which acts similarly to the strong force in QCD. The total mass of the proton or neutron can then be expressed as:

$$m_N = \sum_{\text{solitons}} \frac{\hbar\omega_{\text{soliton}}}{c^2} + \int \lambda_{\text{coupling}} |\phi|^2 |\Psi|^2 d^3x \quad (53)$$

This accounts for the contribution from the soliton's rest mass and the binding energy from the soliton-phonon interactions.

Phonons (which represent both gluons and photons) act as massless energy carriers and are responsible for distributing energy rather than holding or keeping energy. Because of this, they do not generate mass. This is similar to how gluons and photons in the Standard Model remain massless while mediating the strong and electromagnetic forces, respectively.

The total mass of a proton or neutron m_N can be described as: $m_N = m_{\text{quarks}} + E_{\text{binding}}$ where E_{binding} is the binding energy due to the strong interaction.

The quark energy (E_{quarks}) comes from their interactions with the scalar field or other fields: $E_{\text{quarks}} = \sum_i \frac{\hbar\omega_{\text{quark},i}}{c^2}$, where $\omega_{\text{quark},i}$ represents the frequency of each quark's oscillation within the scalar field or BEC.

The binding energy (E_{binding}) comes from the interactions between quarks, mediated by phonons (representing gluon-like interactions): E_{binding} (quark-phonon) $\sim \int \lambda_{\text{coupling}} |\phi|^2 |\Psi|^2 d^3x$

where ϕ is the quark field, Ψ is the phonon (BEC) field.

Thus, the total mass of the proton or neutron can also be expressed as a QCD-like model as:

$$m_N \approx \sum_{\text{quarks}} \frac{\hbar\omega_{\text{quark}}}{c^2} + \int \frac{1}{4} G^{\mu\nu} G_{\mu\nu} d^3x \tag{54}$$

where; $\sum_{\text{quarks}} \frac{\hbar\omega_{\text{quark}}}{c^2}$ represents the rest mass contributions from the valence quarks in the nucleon, $\int \frac{1}{4} G^{\mu\nu} G_{\mu\nu} d^3x$ represents the energy density from the gluon fields that bind the quarks, and $G^{\mu\nu}$ is the gluon field strength tensor in QCD, which captures their interactions.

5.2 **W and Z bosons.**

The roton differs from the phonon because it has a unique ability to concentrate energy density. Phonons are low-energy, long-wavelength excitations at small momentum values. Rotons occur at higher momentum values and are short-wavelength oscillations. This distinction between rotons and phonons creates a roton energy gap [102], the minimum energy needed to excite a roton. This sits at a finite energy level above phonon energies. The roton can be viewed as a localized excitation within the BEC with a finite energy gap. This energy gap is related to the mass

of the W and Z bosons. The concentration of energy density around the roton means it holds energy that can be associated with mass. The energy of the roton can be written as:

$$E_{\text{roton}} = \sqrt{(\hbar\omega_{\text{roton}})^2 + (mc^2)^2} \tag{55}$$

where; ω_{roton} is the frequency of the roton's oscillation, m is the mass associated with the roton that corresponds to the W or Z boson**.** The masses of the W and Z bosons after symmetry breaking are given as:

$$m_W = \frac{gv}{2} \quad , \; m_Z = \frac{gv}{2\cos\,\theta_W} \tag{56}$$

where; g is a weak coupling constant, θ_W is the Weinberg angle.

There exists a “Roton Energy Gap” which can be explained as follows:

At low momenta, the dispersion is linear, which describes the phonons: $E_{\text{phonon}}\,(p) \approx c_s p$

The dispersion curve flattens at higher momenta and reaches a minimum at a finite momentum value. This region describes the roton, and a finite energy gap is required to create a roton excitation within the superfluid. This can be shown as:

$$E_{\text{roton}}\,(p) = \Delta + \frac{(p-p_0)^2}{2m^*} \tag{57}$$

where; Δ is the energy gap between phonons and rotons, p_0 is the momentum at which the energy of the roton is minimized, m^* is an effective mass associated with the roton, which plays an essential role in the roton's interaction strength and propagation characteristics as a quasi-particle.

5.3 **Neutrinos.**

Neutrinos [103] have spin but no charge and play no direct role in matter formation. In this model, they are generated via the cyclic energy exchanges between the scalar and BEC fields, serving the role of energy-dissipation quanta. They are believed to be the residual kinetic energies leftover from soliton, phonon, and roton interactions. The different flavors of neutrinos (electron, muon, tau) could correspond to different angular momentum modes or configurations in the energy transfer process. As neutrinos travel, they change flavor through neutrino oscillations. This flavor change could be a natural consequence of how angular momentum is transferred in this energy exchange. This might be due to asymmetry in the scalar field-BEC interaction that favors left-handed configurations for these particles.

Neutrinos interact via the weak nuclear force, mediated by W and Z bosons. The weak interaction is much weaker than the electromagnetic or strong interactions, so neutrinos can pass through vast amounts of matter (like the Earth) without interacting with other particles.

An equation representing the kinetic energy feedback loop in the scalar field and decay process could take the form as: $E_{\text{kinetic}}(t) \propto E_0 \cdot \sin(\omega t) \cdot e^{-\gamma t}$ where E_0 is the initial kinetic energy, ω is the frequency of oscillations, γ represents the decay rate, which could correspond to the lifetime of the particles (muons or tau neutrinos).

The feedback loop maintains energy conservation through the oscillatory decay of kinetic energy:

$$E_{\text{total}} = E_{\text{kinetic}}(t) + E_{\text{muons / tau particles}}(t) \tag{58}$$

$$E = \hbar\omega \qquad \begin{aligned} \omega_{\text{muon}} &= \frac{E_{\text{muon}}}{\hbar} \approx 1.6 \times 10^{22}\text{rad/s} \\ \omega_{\text{tau}} &= \frac{E_{\text{tau}}}{\hbar} \approx 2.7 \times 10^{23}\text{rad/s} \end{aligned}$$

The weak interaction between neutrinos and the boson field can be described by:

$$\mathcal{L}_{\text{weak}} = g_W \bar{\nu}_L \gamma^\mu A_\mu \nu_L \tag{59}$$

Where; $\bar{\nu}_L$ and ν_L represent the left-handed neutrino fields, A_μ is the boson field representing weak interactions, g_W is the weak coupling constant. Neutrinos interact very weakly with the boson field, so they are unaffected by the Higgs mechanism and possess a low mass.

6. **Stress- Energy-Momentum Tensors**.

The transition of energy waves through the scalar field, the cyclic exchanges between the scalar and BEC, plus interactions within the BEC superfluid can generate stress-energy-momentum tensors [104] on the lower two-dimensional (spacetime) boundary. The energy-momentum tensor $T_{\mu\nu}$ encapsulates the distribution of this energy and momentum in spacetime.

Stress-Energy Tensor of the Scalar Field can be written as:

$$T_{\mu\nu} = \partial_\mu \phi \, \partial_\nu \phi - g_{\mu\nu} \left(\frac{1}{2} g^{\alpha\beta} \, \partial_\alpha \phi \, \partial_\beta \phi + V(\phi) \right) \tag{60}$$

where; $T_{\mu\nu}$ is the stress-energy tensor for the scalar field ϕ describing how the scalar field's energy and momentum affect spacetime's curvature, $\partial_\nu \phi$ is the derivative representing how the scalar field changes to the spacetime coordinate x^ν , $g_{\mu\nu}$ is the metric tensor describing the geometric properties of spacetime, $g^{\alpha\beta} \partial_\alpha \phi \partial_\beta \phi$ is the kinetic energy density of the scalar field,

and $g^{\alpha\beta}$ is the (inverse metric tensor) that contracts the derivative of the scalar field to account for the spacetime curvature.

Within the BEC superfluid, the oscillatory effects leading to density waves and vortex formations contribute to its stress-energy tensor $T_{\mu\nu}$ given as:

$$T_{\mu\nu} = \rho u_\mu u_\nu + p\left(g_{\mu\nu} + u_\mu u_\nu\right) + \tau_{\mu\nu} + S_{\mu\nu} + \eta\omega_{\mu\nu} \tag{61}$$

where; ρ is the energy density, p is the pressure, $\tau_{\mu\nu}$ is the shear stress tensor, which includes contributions from angular momentum and vortex formation, $g_{\mu\nu}$ is the metric tensor, u_μ is the four-velocity, $S_{\mu\nu}$ represents the contribution from angular momentum and momentum flux. It encodes the transport of angular momentum and can be linked to the system's vorticity or circulation as: $S_{\mu\nu} = \frac{1}{2}\left(J_\mu v_\nu + J_\nu v_\mu\right)$ where J_μ is the angular momentum density in the direction μ corresponding to the rotation or vorticity in the system, v_ν is the velocity field or four-velocity associated with the rotational flow and $J_{\mu\nu}$ is the angular momentum flux, $\omega_{\mu\nu}$ is a vorticity tensor; $\omega_{\mu\nu} = \partial_\mu u_\nu - \partial_\nu u_\mu$ shows how the rotational motion in the BEC induced by the solitons contributes to the overall momentum flux and stress-energy tensor, and η is a coupling constant. These interactions lead to frame-dragging effects forming spacetime (lower boundary). According to Einstein's general relativity, the curvature of spacetime is determined by the stress-energy content, which is described by Einstein's field equations as:

$$G_{\mu\nu} = 8\pi G T_{\mu\nu} \tag{62}$$

where $G_{\mu\nu}$ is the Einstein tensor representing the curvature of spacetime. This equation links the stress-energy tensor $T_{\mu\nu}$ to the curvature of spacetime. As energy and momentum are exchanged

in the scalar and BEC fields, the stresses generated warp its lower two-dimensional boundary, eventually forming a spacetime curvature. This can be further described as:

$$T_{\mu\nu}^{\text{boundary}} = \frac{1}{8\pi G_N} \lim_{r \to R_{\text{BEC}}} r^2 g_{\mu\nu}^{\text{scalar-BEC}} \tag{63}$$

where; $T_{\mu\nu}^{\text{boundary}}$ is the stress-energy tensor on the lower-dimensional boundary, G_N is Newton's gravitational constant, $r \to R_{\text{BEC}}$ is the radial coordinate r approaching the radius of the (BEC) system, which defines the bulk-boundary interaction zone, $g_{\mu\nu}^{\text{scalar-BEC}}$ is the induced metric on the boundary.

7. **Cosmic Microwave Background (CMB).**

The CMB, discovered in 1965, relays the early Universe's thermal past. Its presence generated the concept of an expanding universe from a hot Big Bang [105]. The CMB is observed today as a nearly perfect Black Body spectrum [106] at about 2.725 K, indicating that its radiation is in thermal equilibrium. The CMB is remarkedly isotropic and homogenous on large scales. It contains small temperature fluctuations or anisotropies on the order of one part in 100,000 ($\Delta T/T \approx 10^{-5}$) with acoustic peaks. In the early universe, Baryonic Acoustic Oscillations (BAO) [107] were responsible for the oscillations that created the temperature fluctuations seen in the CMB. However, presented here is an alternative explanation of the features of the CMB without needing an inflationary [108] Big Bang. Interactions within superfluids, despite being frictionless, have been shown to generate heat [109].

The many stress-energy tensors $T_{\mu v}$ generated by soliton, phonon, roton, and vortex ring interactions within the BEC produces thermal radiation or dissipative heating, which exits as the CMB. This is shown as:

$$Q_{\text{heat}} = \int T_{\mu v}\, \partial_v \phi d^3x \tag{64}$$

where Q_{heat} is the part of the energy released as radiation. Thermal equilibrium is achieved through phonon-phonon long-wave excitations, generating a Black Body type spectrum. This can be shown as:

$$f(E) = \frac{1}{e^{E/k_B T} - 1} \tag{65}$$

where; E is the energy of the phonon modes, k_B is the Boltzmann's constant, and T is the temperature of the system.

Phonons, as long-range acoustic collective excitations, are propagated in much the same way as BAOs of the CMB, which are energy density perturbations**.** The fluctuations in density can then create the temperature anisotropies**.** The power spectrum $P(k)$ for the phonon field shows the distributions of the wave amplitude fluctuations across different wave numbers k which could be modeled as: $P(k) \sim \langle |\delta\Psi_{\text{phonon}}(k)|^2 \rangle$, where $\delta\Psi_{\text{phonon}}(k)$ captures the phonon density perturbations, which help explain structure formation in the universe.

High phonon density (regions of constructive interference) creates hot spots, and low phonon density (regions of destructive interference) produces cold spots. This can be modeled by a phonon field Ψ_{phonon} wave equation as:

$$\frac{\partial^2 \Psi_{\text{phonon}}}{\partial t^2} - c_s^2 \nabla^2 \Psi_{\text{phonon}} = 0 \tag{66}$$

where; $\nabla^2 \Psi_{\text{phonon}}$ is the Laplacian describing spatial variations, c_S is the speed of sound in the superfluid.

The thermal excitations generated within the BEC are carried in a second thermal sound wave as oscillations of the superfluid medium. The second sound is a thermal wave that propagates in superfluids [110], particularly in superfluid helium and Bose-Einstein condensates. The first sound would correspond to the acoustic waves responsible for Baryon Acoustic Oscillations (BAO). The second sound would represent the thermal radiation from the CMB, where temperature variations in the CMB correspond to oscillations in the entropy of the superfluid (BEC). In superfluids, the second sound is governed by the following equation:

$$\frac{\partial^2 T}{\partial t^2} = v_{\text{SS}}^2 \nabla^2 T \tag{67}$$

where; T is the temperature (corresponding to CMB temperature fluctuations), v_{SS} is the speed of a second sound, ∇^2 represents the Laplacian operator for spatial derivatives.

The CMB would then represent the fossil imprint of these second sound waves, with the temperature anisotropies in the CMB directly related to the propagation of these thermal waves through the quantum superfluid (BEC).

As the superfluid expands or evolves, the energy density decreases, cooling the radiation emitted by the system. This process would mimic the redshift and cooling of the CMB radiation as the universe expanded. The CMB can be modeled as a quantized field of photons produced by these interactions:

$$T_{\mathrm{CMB}} = \left(\frac{E_{\text{soliton-phonon}}}{V}\right)^{\frac{1}{4}} \tag{68}$$

8. **Dark Energy and the Hubble Tension.**

One of the characteristics of light waves traversing a BEC medium is their velocity slows [111]. The lost kinetic energy does not disappear but is redistributed into the potential energy $V(\Psi)$ of the BEC. The wavefunction Ψ of the BEC changes as a result of this energy transfer, which causes it to experience pressure that behaves inversely to typical pressure —negative pressure. This leads to expansion forces within the BEC [112]. These features are mirrored by pathway B of the dark energy beam, which triggers an expansive negative pressure within the BEC medium.

The pressure P in a BEC-like system can be described as a function of the Lagrangian density $\mathcal{L}$, which includes both the kinetic and potential energy contributions:

$$P = -\left(\frac{\partial \mathcal{L}}{\partial g_{\mu\nu}}\right) \tag{69}$$

In this case, where the kinetic energy contribution is minimal (as light slows down), the potential energy dominates, and we can approximate: $P \approx -V(\Psi)$

Thus, the pressure becomes negative, proportional to the potential energy $V(\Psi)$ of the BEC. The negative pressure induced by the interaction between the dark energy beam and the BEC superfluid causes the space between the density perturbations in the BEC to expand. This expansion can be described by the Friedmann equation [113] as:

$$\left(\frac{\dot{a}}{a}\right)^2 = \frac{8\pi G}{3}\rho_{\text{total}} - \frac{k}{a^2} \tag{70}$$

where; a is the scale factor, $\dot{a}$ is the time derivative of the scale factor a , ρ_{total} is the energy density contributions from the dark energy and the BEC, k is the spatial curvature, which is zero for a flat universe.

The relationship between the pressure P and the energy density ρ of dark energy can be described by its equation of state w: $w = \frac{P}{\rho}$, P is negative and equal in magnitude to the energy density ρ: $P = -\rho$, $w = -1$, which corresponds to the model's cosmological constant-like [114, 115] behavior for dark energy, resulting in cosmic expansion.

The second law of thermodynamics states that the entropy of a closed, isolated system must increase over time [116]. Entropy begins very low and increases through CMB and cosmic radiation losses. This means the universe has been losing energy to radiation since its inception.

However, there must be a balance in energy conservation:

$$E_{\text{total}} = E_{\text{kinetic}} + E_{\text{BEC}} + E_{\text{scalar}} + E_{\text{radiation}} = \text{constant}$$

$$E_{\text{total}} = E_{\text{kinetic}}(t) + \int \left(\frac{1}{2}(\nabla\phi)^2 + V(\phi) + \frac{1}{2}(\nabla\Psi)^2 + V_{\text{BEC}}\right) d^3x + E_{\text{radiation}} \quad (71)$$

Dark energy achieves this through an accelerated expansion of the universe, compensating for the long period of energy loss as the redshifting of radiation as space expands. The energy density of the radiation ($\rho_{\text{radiation}}$) scales with the expansion factor $a(t)$ **,** as: $\rho_{\text{radiation}}(t) \propto \frac{1}{a(t)^4}$

This accelerated expansion keeps the overall energy balance intact by stretching space and distributing the remaining energy across a larger volume. This means that dark energy contributes a constant (or slightly increasing) energy density that pushes the universe to expand

without being diluted. This is consistent with the dark energy theory presented here, allowing it to have a nearly constant energy density as: $\rho_{\text{dark energy}} \propto \Lambda$.

Dark energy observations showed it only became dominant 9 billion years later [117], consistent with the model's late arrival of dark energy's beam B to the lower boundary, allowing for early galaxy formation.

8.1 **A Solution to the Hubble Tension.**

The phonon waves within the BEC drove the Universe's early expansion and the formation of structures such as galaxies, allowing for a lower Hubble constant H_0 in the early universe as shown by:

$$H(t)^2 = \frac{8\pi G}{3}\left(\rho_{\text{BEC}} + \rho_{\text{scalar}} + \rho_{\text{radiation}} + \rho_{\text{dark energy}}\right)$$

For the early universe: $H_{\text{early}}(t)^2 = \frac{8\pi G}{3}\left(\rho_{\text{matter}}(t) + \rho_{\text{radiation}}(t)\right)$ (72)

$H(t)$ is the Hubble parameter, which defines the rate of expansion. Measurements from the CMB and BAO give a $H_0 \approx 67\text{km/s/Mpc}$. Here, the contribution of dark energy is small or delayed.

However, measurements from supernovae observations $H_0 \approx 73\text{km/s/Mpc}$ are larger because of the late contributions from dark energy.

For the late universe: $H_{\text{late}}(t)^2 = \frac{8\pi G}{3}\left(\rho_{\text{matter}}(t) + \rho_{\text{radiation}}(t) + \rho_{\text{dark energy}}(t)\right)$ (73)

Hence, the Hubble tension dilemma becomes non-existent as measurements are consistent with the model's predictions.

9. **Holographic Interference Patterns and Time.**

The two dark energy pathway beams, A and B, behave similarly to a hologram's object and reference beams. Pathway A, containing all the waveforms generated from soliton and phonon interactions, becomes the object beam, and pathway B, containing the observer, acts as the reference beam. Their interaction collapses the wave information into a 2D holographic interference pattern on the lower-dimensional boundary of the dark matter field. The interference forms a diffraction grating [118], where the wavefunctions of the solitons, phonons, and their interactions with the CMB first and second waves are projected and encoded. The interference pattern can be represented as a superposition of wavefunctions from the object and reference beams. Mathematically, shown as:

$$I(x) = \left|\phi_{\text{object}}(x) + \phi_{\text{ref}}(x)\right|^2 \tag{74}$$

where; $\phi_{\text{object}}(x)$ is the wavefunction from the object beam, and $\phi_{\text{ref}}(x)$ is the wavefunction from the reference beam (dark energy with the observer), $I(x)$ is the interference term that encodes the universe's fields as a hologram.

Gravity becomes the warping of the lower boundary as curved spacetime, where the wave information is encoded as a holographic diffraction pattern. The following equation illustrates this:

$$G_{\mu\nu} = \frac{8\pi G}{c^4}\left(T_{\mu\nu}^{\text{holographic}} + T_{\mu\nu}^{\text{curvature}}\right) \tag{75}$$

where; $T_{\mu\nu}^{\text{holographic}}$ is the stress-energy tensor for the holographically projected fields**,** $T_{\mu\nu}^{\text{curvature}}$ represents the stress-energy from the curvature of the lower boundary.

The movement of the reference beam (dark energy with the observer) introduces time [119] into the system. As the reference beam shifts, it alters the interference pattern, leading to a time-dependent evolution of the fields on the boundary. A time-evolution operator can represent this, $U(t)$ acting on the wavefunction fields Ψ:

$$\Psi(t) = U(t)\Psi(0) = e^{iHt/\hbar}\Psi(0) \tag{76}$$

Where *H* is the Hamiltonian governing the dynamics of the soliton-phonon system, describing the evolution of the holographic fields as the flow of time.

The Fourier transform of the interference patterns [120] can model the emergence of time:

$$\mathcal{J}(t) = \sum_k e^{i\omega_k t}|\Psi_k|^2 \tag{77}$$

This equation describes the interference pattern on the boundary as a superposition of quantum states k where; $\mathcal{J}(t)$ is a time-dependent interference term, the exponential $e^{i\omega_k t}$ captures the oscillatory phase associated with each state k where ω_k is the angular frequency modes of the solitons and phonons, and t emerges as a parameter associated with the evolution of these modes on the boundary. The periodic nature of these modes generates the illusion of time, which could be interpreted as a coordinate on the lower-dimensional boundary and emerging as holographic time.

9.1 **Holographic Time Dilation.**

Time dilation [121] depends on the curvature of the boundary, which encodes the gravitational effects. The closer you are to the boundary, the stronger the curvature and time slows. This relationship could be expressed as:

$$\frac{\Delta t_{\text{far}}}{\Delta t_{\text{near}}} = \sqrt{1 - \frac{k}{r^2}} \tag{78}$$

where; Δt_{far} is the time interval far from the mass (or boundary), Δt_{near} is the time interval close to the mass (or boundary), k is a constant that depends on the curvature of the boundary (related to the stress-energy tensor), r is the distance from the boundary. This equation expresses the emergent time.

9.2 **Holographic Light Bending.**

In this holographic model, the bending of light near the curved boundary can be expressed as:

$$\theta = \frac{k}{r^2} \tag{79}$$

where; k is a constant that depends on the curvature of the boundary, r is the distance from the object (or boundary). This equation shows that light bending near the curved boundary is similar to how light bends around massive objects in General Relativity.

10. **Conservation of Energy and Angular Momentum**

The following equation describes energy conservation [122] in the model:

$$\nabla_\mu T^{\mu\nu} + \frac{d}{dt}\int_V \left(\epsilon_{ijk} x^j T^{0k}\right) d^3x = 0 \tag{80}$$

$\frac{d}{dt}\int_V (T^{00}) d^3x = 0$ (Energy conservation)

$\frac{d}{dt}\int_V \left(\epsilon_{ijk} x^j T^{0k}\right) d^3x = 0$ (Angular momentum conservation)

where; T^{00} is the energy density of the system, T^{0k} is the momentum density, ϵ_{ijk} is the Levi-Civita symbol.

11. **Quantization of the Fields and Spacetime Geometry**

(a) The total Lagrangian density for Soliton-Phonon-Roton Interaction is shown by:

$$\mathcal{L} = \frac{1}{2}\left(\partial_\mu \hat{\phi}\partial^\mu \hat{\phi} + \partial_\mu \hat{\Psi}\partial^\mu \hat{\Psi} + \partial_\mu \hat{R}\partial^\mu \hat{R}\right) - V(\hat{\phi}, \hat{\Psi}, \hat{R}) - \lambda\hat{\phi}\hat{\Psi} \tag{81}$$

where; $\hat{\phi}, \hat{\Psi}, \hat{R}$ are the quantized fields for soliton, phonon, and roton, respectively, $\lambda\hat{\phi}\hat{\Psi}$ represents the quantum interaction between soliton and phonon fields, $V(\hat{\phi}, \hat{\Psi}, \hat{R})$ is the potential energy term governing the self-interactions of these fields.

(b) Interaction Between Fields and Boundary (Holographic Interaction):

$$\mathcal{L}_{\text{boundary}} = \int_{\text{boundary}} d^3x\left(\hat{\phi}_{\text{boundary}}\, \hat{\Psi}_{\text{boundary}}\, \hat{R}_{\text{boundary}}\right) \tag{82}$$

(c) Commutation Relations for Quantum Fields:

$$\begin{aligned}
\left[\hat{\phi}(x), \hat{\pi}_\phi(x')\right] &= i\hbar\delta(x - x') \\
\left[\hat{\Psi}(x), \hat{\pi}_\Psi(x')\right] &= i\hbar\delta(x - x') \\
\left[\hat{R}(x), \hat{\pi}_R(x')\right] &= i\hbar\delta(x - x')
\end{aligned} \tag{83}$$

For each of the fields—soliton ($\hat{\phi}$) phonon ($\hat{\Psi}$) , and roton ($\hat{R}$) canonical commutation relations are imposed to describe the quantum nature of these fields. The conjugate momenta $\hat{\pi}_\phi, \hat{\pi}_\Psi, \hat{\pi}_R$ are the canonical momenta associated with each field.

(d) Quantized Stress-Energy Tensor:

$$\hat{T}_{\mu\nu} = \partial_\mu \hat{\phi} \partial_\nu \hat{\phi} + \partial_\mu \hat{\Psi} \partial_\nu \hat{\Psi} + \partial_\mu \hat{R} \partial_\nu \hat{R} - g_{\mu\nu} \mathcal{L} \tag{84}$$

This tensor operator $\hat{T}_{\mu\nu}$ defines how the energy, momentum, and stress are distributed within quantum fields across spacetime, where $g_{\mu\nu}$ is the metric tensor defining distances in spacetime and $\mathcal{L}$ is the Lagrangian density of the fields. $\hat{T}_{\mu\nu}$ is used in Einstein's field equations on the boundary as:

$$R_{\mu\nu} - \frac{1}{2} g_{\mu\nu} R = 8\pi G \langle \hat{T}_{\mu\nu} \rangle \tag{85}$$

where $\langle \hat{T}_{\mu\nu} \rangle$ is the expectation value of the quantized stress-energy tensor.

(e) Emergence of Quantum Fields from Interference Pattern (Holographic QFT):

$$\hat{I}(x) = |\hat{\phi}(x) + \hat{\Psi}(x) + \hat{R}(x)|^2 \tag{86}$$

The interference pattern $\hat{I}(x)$ describes how the quantum fields interact and interfere on the boundary. The quantum fields are projected from this interference pattern, reconstructing the bulk QFT fields. Fermions arise from soliton interactions, bosons from phonon interactions, the Higgs-like field provides mass through symmetry breaking, and the gluon-like field confines quarks and produces hadrons.

(f) Spacetime Curvature as the "Emergent Geometry" can be given by a holographic boundary version of Einstein's field equation as:

$$R_{\mu\nu}^{\text{boundary}} - \frac{1}{2} g_{\mu\nu}^{\text{boundary}} R^{\text{boundary}} = 8\pi G \langle \hat{T}_{\mu\nu}^{\text{boundary}} \rangle \tag{87}$$

where $\langle \hat{T}_{\mu\nu}^{\text{boundary}} \rangle$ is the expectation value of the stress-energy tensor on the boundary, which accounts for the stress-energy momentum from the fields that influence the boundary curvature.

This links the quantum fields to the curvature of spacetime and the bulk geometry [123, 124]. The emergent spacetime curvature is a reflection of the underlying quantum field curvature.

11.1 **The measurement problem and wave-particle duality.**

The Schrödinger equation [125] describes how a wavefunction's system evolves, with its quantum information in a superposition of all possible states. Only when a measurement is carried out does the wavefunction collapse [126] into a single definite outcome. A measurement can be any interaction with the system, whether as a direct observer or via instrumentation. The central issue is the wave collapse, which, based on the model presented here, is believed to be a wrong interpretation. What is posited is that all forms of matter are waves. In reality, particles such as fermions and bosons are quantized versions of solitons and phonons, which are waveforms. There is no wave collapse; the observer or interacting system causes an excitation within the underlying field's wavefunction, which is seen as a point-like particle. Yes, in this model, observation can excite the field. Essentially, there is no wave-particle duality. An electron, for example, exists not as a single isolated particle as the total collapse of the wave's information but as an excitation within its underlying fermion field. Hence when it passes through one or both slits of the double-slit experiment, it always passes as a wave and never as a particle. When a measurement is performed anywhere along its trajectory, it excites the fermion field, generating the electron that appears on the screen as a point. Hence, there is no loss of quantum information. An electron can appear as existing in two places at once because it is simply an

excited state of its underlying field and will appear wherever a measurement or observation occurs.

11.2 **Quantum Entanglement.**

Similarly, two entangled electrons exist as excitations within their shared fermion field. Separating them does not change the fact that the underlying fermion field still connects them. Hence, any measurement of one immediately changes the other. Information cannot travel faster than the speed of light. However, in the model, the interacting electrons are quantized holographic images of solitons; the real entanglement occurs in a higher dimension where time does not exist. Hence, any entangled system exchanges information without time constraints and happens instantaneously.

11.3 **Matter-antimatter asymmetry.**

In this model, charge-parity symmetry [127] becomes broken for several reasons, beginning with the scalar field's transition from linear to non-linear symmetry. The asymmetric cyclic energy exchanges between the scalar and BEC fields and the soliton and phonon interactions favor more significant soliton-like matter generation than anti-soliton. The increasing entropy and energy dissipation also created asymmetries, resulting in a bias for stable, long-standing matter solitons over antimatter.

12. **The cosmic web**

This represents the entangled kinetic energy distribution within the BEC superfluid and its emergence within the quantized fields. High-density regions lead to the formation of galaxy clusters and filaments. Low-density regions without entanglement result in cosmic voids, where little to no matter exists and are seen as cold spots in the CMB. This can be represented as:

$$\delta\rho(\mathbf{x}) = \int \mathcal{E}(\mathbf{k}, t) e^{i\mathbf{k}\cdot\mathbf{x}} d^3k \tag{88}$$

where; $\delta\rho(\mathbf{x})$ represents the density perturbation that leads to the formation of the cosmic web, $\mathcal{E}(\mathbf{k}, t)$ represents the distribution of kinetic energy in the entangled mesh, k is the wave vector representing the spatial variation of the energy field.

Our Universe's cosmic web describes an interplay between holographic dark energy and dark matter [128].

Consciousness (pathway B)

Upon entering the BEC, beam B of dark energy becomes entangled with the Observer carrying it within its streams. As the dark energy travels in its downward trajectory, it loses kinetic energy, which is transferred as an increase in the potential energy of the BEC medium. As mentioned earlier, this is a feature of the passage of light within a BEC. During this slow transition phase, all the information initially depicted as geometric shapes and forms to the Observer becomes decoded into aspects of "Self" [129]. Every conceptual Self then becomes an archetype representing its unique features and attributes. These prototypes are static waveforms within

the BEC superfluid. However, as the energy beams penetrate each archetype, they disperse into smaller streams, generating multiple miniature animated forms of a similar likeness. This creates many structures resembling animal and plant-like shapes as versions of what the Observer can be as a Self. The system has a hierarchical order, with the human form as supreme. Though this may resemble the story of Genesis [130], it has nothing to do with religion; it is simply the coding and decoding of self-generated information, such as the human genome. All geometric forms exist as optical waves. The convoluted light networks assume residence within structures with a head cavity as a reductive form of its higher dimensional entangled network. This is analogous to the human brain's neural network, and their similarity can be drawn. Beam B continues branching like a tree-like network as it travels to the 2D lower-dimensional boundary. There, it acts as an object beam, generating a holographic interference pattern with the reference beam of pathway A. The optical diffraction grating formed on the lower 2D boundary encodes the wave information of beam B. As beams A and B continue their interference, serving as each other's object and reference beams, they create a multilayered diffraction grating, decoded as a reconstructed 3D hologram of classical information. A Universe of classical forms appears as excitations within the projected holographic quantum fields.

Concerning the human form, the human brain's neural network represents its higher dimensional light-energy network within its comparable optical form. The dynamic patterns within these higher optical brain-like networks are the originators of thought, imagery, memory, and emotions as attributes of their innate nature. Their multi-colored nature also explains why our mood and affect are influenced by color despite the human brain's matter having no color receptors. It is also why color perception is generated from neural activity, even though the inside

of a human skull is dark. The hard problem of consciousness involves the concept of an inner experiencer or self, which differs from the outer material body. It is defined as, “What’s it like to be me?” In his book, “What’s it like to be a bat?”[131], Thomas Nagel captures that experiences are unique to the organism. Neuroscience has been unable to explain how neuronal matter can generate rich experiences as qualia [132], such as the taste of chocolate, the feeling of awe, and the experience of redness of red. Experiments have not been able to reproduce these self-experiences as the Neural Correlates of Consciousness [133]. In this theory’s framework, consciousness can arise from the Observer alone. It is the sole interpreter of the information generated from the patterns of energy movements within the neuronal net. The organism can only see, experience, and feel through the Observer's presence. Individual subjectivity arises from the energy flux within the optical neural net of each unique form. It is why our neural network is individualized, similar to a fingerprint. The Observer is universal without subjectivity. The inner self is, therefore, always present in wakefulness and dreams when there is neural activity, vanishing when it is at its minimal ground state, as in deep sleep. The Observer does not enter the brain’s neural net but resides at its “doorstep” within the brain stem's Ascending Reticular Activating System (ARAS) [134], which is extensively connected to higher cortical centers. For this reason, even individuals with a significant loss of neocortical function can still have conscious experiences [135], though the content of the experience may be limited. Even the ARAS's tiniest lesions can completely obliterate all forms of consciousness [136]. In neuroscience, wakeful awareness [137] resides solely within the ARAS, and in the model presented, it is due to the Observer’s presence.

The Observer's role as the “knower” remains within its higher dimensional forms. However, its conscious influence is recreated within the holographic avatar-like composites. Brain injury can produce diminished consciousness because the ability to generate and transmit the informational content of experiences within the network to the Observer is hampered. The presence of the conscious Observer and the movement of its energy generated by pathway B can produce forms of matter that are said to be “alive.” This contrasts with forms produced from pathway A, in which the Observer’s presence is absent, and the matter is said to be dead. In summary, our conscious experiences are a product of the Observer’s presence and the informational content generated by its energy flux.

Discussion

This unified theory, grounded in the interactions between scalar fields, solitons, phonons, and Bose-Einstein Condensates, offers a novel approach to solving some of the most pressing challenges in modern physics and cosmology. By merging quantum mechanics and general relativity, the theory provides a new framework for understanding the curvature of spacetime, dark energy, dark matter, gravitational waves, the formation of black holes, and the Observer’s role in consciousness. The emergence of time and quantum fields from solitonic vibrations introduces a new way of conceptualizing the flow of energy and the Universe's structure, potentially addressing anomalies like the Hubble tension, matter-antimatter asymmetry, and the early universe’s supermassive black holes and galaxies.

Here is a summary of a few of the model's predictions: Gravity may not have a quantized state as a graviton; spacetime exists as the curvature of the lower dimensional boundary of the dark matter field; there may be no primordial gravitational waves; the dark matter field is not a particle, existing everywhere as a BEC-like superfluid; black holes may not have a singularity; SMBHs are an early feature before galaxy formation; there are many other quasi-particles and exotic forms of matter; the Universe is a holography of waveforms; there exists a higher dimension from which our dimension emerges; the cosmic web and brain's neural net are mirror images of a higher dynamical dark energy network; the expansion of the universe will eventually slow as energy conservation is restored, time is a Fourier transformation of HIPs waveforms, the Hubble tension is non-existent; the fine structure constant has a composite structure; dark energy and matter are holographic features of our Cosmos and exist only in a higher dimension, the CMB is the thermal relic of a second sound wave, an electron and proton are quantized versions of a soliton and a vortex ring, hence the simplest structure will be an abundance of hydrogen; and the model also suggests more matter than anti-matter with the Universe being spatially flat.

This framework opens new avenues for exploration, offering theoretical and experimental implications for understanding the fundamental nature of reality. Future work will involve testing the theory's predictions in both quantum and cosmological contexts. Implementing numerical simulations can help validate the theoretical predictions. Simulations can model the creation of entangled soliton pairs and their interactions with phonon modes, generate holographic interference patterns, density perturbations, and black hole analogs. Experimentally, ultracold atomic gases can be used to create BEC modes that can induce soliton and dark soliton formation

through controlled perturbations, observe soliton-phonon interactions, and employ advanced imaging techniques to visualize HIPs. Cosmological observations to substantiate the theory can analyze the statistical properties of CMB-like anisotropies and examine galaxy distribution patterns, BAO signatures, and gravitational wave emissions as correlations to the model.

Future work can involve harnessing consciousness' entangled nature and linking it to quantum processes in quantum computing, incorporating observer-conscious interactions into quantum algorithms, and mimicking how consciousness interacts with quantum fields. The theory's reliance on holographic principles could inspire the development of holographic data storage and retrieval systems capable of encoding information in complex interference patterns, allowing vast amounts of data to be stored in highly compact forms. Since the theory revolves around BEC superfluidity, this might lead to advancements in energy-efficient transport systems, where superfluid technologies could minimize energy loss. This could revolutionize industries such as power grids and quantum energy networks, where energy can be moved without resistance to create new frictionless transport technologies for space exploration. Understanding negative pressure and dark energy could lead to novel propulsion systems. By manipulating negative pressure, new forms of spacecraft propulsion could be designed, potentially enabling faster-than-light travel or highly efficient interstellar travel by harnessing dark energy-like properties. The theory could lead to developing technologies capable of tapping into the vacuum or zero-point energy fields, unlocking new energy sources. This would be revolutionary for energy generation, offering virtually limitless clean energy by harnessing the fundamental interactions of dark energy and quantum fields. The theory suggests that gravity emerges from quantum (solitons) interactions; it could lead to technologies that allow for the manipulation of gravitational fields.

This could revolutionize industries such as aerospace, enabling anti-gravity or gravity-shielding technologies, which could drastically reduce energy costs for launching spacecraft. Quantum sensors that leverage the entanglement of solitons and phonons within a superfluid framework could offer far greater sensitivity than current technologies, revolutionizing fields such as medical diagnostics and environmental monitoring. The theory's integration of consciousness with quantum fields could inspire the creation of artificial intelligence systems incorporating elements of quantum consciousness. This could open the door to non-invasive quantum healing technologies, where diseases are treated by manipulating quantum fields in the body.

In conclusion, this unified framework deepens our understanding of the cosmos and ourselves. More importantly, it highlights the true nature of reality and the fact that we, the human species, are connected to everything within the Cosmos.

References

1. J. M. Hill, On the formal origins of dark energy. *Z. Angew. Math. Phys.* **69** (2018).
2. G. Bertone, D. Hooper, History of dark matter. *Rev. Mod. Phys.* **90** (2018).
3. C. Koch, What is consciousness? *Nature* **557**, S8–S12 (2018).
4. P. Dirac, *The principles of quantum mechanics*, 4th Ed. (Clarendon Press, 1981).
5. A. Einstein, "The general theory of relativity" in *The Meaning of Relativity*, (Springer Netherlands, 1922), pp. 54–75.
6. W. N. Cottingham, D. A. Greenwood, *An introduction to the standard model of particle physics*, 2nd Ed. (Cambridge University Press, 2023).
7. P. J. E. Peebles, *Principles of physical cosmology* (Princeton University Press, 2020).

8. B. P. Abbott, *et al.*, Observation of gravitational waves from a binary black hole merger. *Phys. Rev. Lett.* **116**, 061102 (2016).

9. C. Kiefer, “Why Quantum Gravity?” in *Approaches to Fundamental Physics*, Lecture notes in physics., (Springer Berlin Heidelberg, 2007), pp. 123–130.

10. R. B. Laughlin, D. Pines, The theory of everything. *Proc. Natl. Acad. Sci. U. S. A.* **97**, 28–31 (2000).

11. S. M. Carroll, *Spacetime and geometry: An introduction to general relativity* (Cambridge University Press, 2019).

12. G. Bertone, The moment of truth for WIMP Dark Matter. *arXiv [astro-ph.CO]* (2010).

13. F. Chadha-Day, J. Ellis, D. J. E. Marsh, Axion dark matter: What is it and why now? *Sci. Adv.* **8**, eabj3618 (2022).

14. P. J. Steinhardt, A quintessential introduction to dark energy. *Philos. Trans. A Math. Phys. Eng. Sci.* **361**, 2497–2513 (2003).

15. P. A. Heelan, “Quantum relativity and the cosmic observer” in *Cosmology, History, and Theology*, (Springer US, 1977), pp. 29–37.

16. M. Pereira, The hypergeometrical universe: Cosmogenesis, cosmology and standard model. *J. Gen. Lie Theory Appl.* **10** (2016).

17. D. Chalmers, “The hard problem of consciousness” in *The Blackwell Companion to Consciousness*, (John Wiley & Sons, Ltd, 2017), pp. 32–42.

18. A. J. Leggett, The quantum measurement problem. *Science* **307**, 871–872 (2005).

19. R. Aldrovandi, A. L. Barbosa, L. C. B. Crispino, J. G. Pereira, Non-relativistic spacetimes with cosmological constant. *Class. Quantum Gravity* **16**, 495–506 (1999).

20. K. Fox, Condensed matter physics: Some like it cold. *Nature* **434**, 430–431 (2005).

21. M. Wadati, Introduction to solitons. *Pramana - J Phys* **57**, 841–847 (2001).

22. L. Reatto, G. V. Chester, Phonons and the properties of a Bose system. *Phys. Rev.* **155**, 88–100 (1967).

23. L. Reatto, D. E. Galli, What is a roton? *Int. J. Mod. Phys. B* **13**, 607–616 (1999).

24. S. Komineas, Vortex rings and solitary waves in trapped Bose–Einstein condensates. *Eur. Phys. J. Spec. Top.* **147**, 133–152 (2007).

25. D. Senderakova, Holography–what is it about.

26. N. Abramson, Light-in-flight recording by holography. *Opt. Lett.* (1978).

27. S. Töpfer, *et al.*, Quantum holography with undetected light. *Sci. Adv.* **8**, eabl4301 (2022).

28. H. A. P. Macedo, L. S. Brito, J. F. Jesus, M. E. S. Alves, Cosmological constraints on $Łambda (t)$CDM models. *Eur. Phys. J. C Part. Fields* **83** (2023).

29. R. Evans, "The cosmic microwave background" in *Astronomers' Universe*, (Springer International Publishing, 2015), pp. 55–89.

30. J. Frieman, M. Turner, D. Huterer, Dark energy and the accelerating Universe. *arXiv [astro-ph]* (2008).

31. J. F. Navarro, The structure of cold dark matter halos. *Symposium* **171**, 255–258 (1996).

32. V. S. Netchitailo, Hubble tension. *Journal of High Energy Physics, Gravitation and Cosmology* **8**, 392–401 (2022).

33. V. Bromm, A. Loeb, Formation of the first supermassive black holes. *Astrophys. J.* **596**, 34–46 (2003).

34. P. Dayal, A. Ferrara, Early galaxy formation and its large-scale effects. *arXiv [astro-ph.GA]* (2018).

35. B. A. Robson, The matter-antimatter asymmetry problem in *Cosmology, Gravitational Waves and Particles*, (WORLD SCIENTIFIC, 2018).

36. M. Sherbon, Fundamental nature of the fine-structure constant. *Int. J. Phys. Res.* (2014).

37. R. Horodecki, P. Horodecki, M. Horodecki, Quantum entanglement. https://doi.org/10.1103/RevModPhys.81.865.

38. R. K. Standish, Why occam's razor. *Found. Phys. Lett.* **17**, 255–266 (2004).

39. D. Walsh, Occam's razor: A principle of intellectual elegance. *Am. Philos. Q.* (1979).

40. E. C. Manavella, Quantum field formalism for the higher-derivative nonrelativistic electrodynamics in 1+1 dimensions. *Int. J. Mod. Phys. A* **34**, 1950050 (2019).

41. R. Banerjee, P. Mukherjee, Subtleties of nonrelativistic reduction and applications. *Nucl. Phys. B.* **938**, 1–21 (2019).

42. M. Heymann, E. Vanden-Eijnden, The geometric minimum action method: A least action principle on the space of curves. *Commun. Pure Appl. Math.* **61**, 1052–1117 (2008).

43. M. S. de Bianchi, The observer effect. *arXiv [quant-ph]* (2011).

44. S. Gielen, D. K. Wise, Lifting general relativity to observer space. *arXiv [gr-qc]* (2012).

45. D. Boulware, L. Brown, Symmetric space scalar field theory. *Annals of Physics* **138**, 392–433 (1982).

46. O. Bergmann, R. Leipnik, Space-time structure of a static spherically symmetric scalar field. *Physical Review* (1957). https://doi.org/10.1103/PhysRev.107.1157.

47. F. Winterberg, Lorentz invariance as a dynamic symmetry. *Z. Naturforsch. A* **42**, 1428–1442 (1987).

48. A. K. Halder, A. Paliathanasis, P. Leach, Noether's Theorem and Symmetry. *Symmetry (Basel)* **10**, 744 (2018).

49. P. A. M. Dirac, "The Lagrangian in quantum mechanics" in *Feynman's Thesis — A New Approach to Quantum Theory*, (WORLD SCIENTIFIC, 2005), pp. 111–119.

50. E. A. Cornell, C. E. Wieman, The Bose-Einstein condensate. *Sci. Am.* **278**, 40–45 (1998).

51. E. Castellanos, C. Escamilla-Rivera, A. Macías, D. Núñez, Scalar field as a Bose-Einstein condensate? *arXiv [gr-qc]* (2013).

52. Q. Zhu, B. Wu, Superfluidity of Bose-Einstein condensates in ultracold atomic gases. *arXiv [cond-mat.quant-gas]* (2015).

53. M. P. Silverman, R. L. Mallett, Dark matter as a cosmic Bose-Einstein condensate and possible superfluid. *General Relativity and Gravitation* (2002). https://doi.org/10.1023/A:1015934027224.

54. A. M. Yao, M. J. Padgett, Orbital angular momentum: origins, behavior and applications. *Adv. Opt. Photonics* (2011).

55. G. Haller, G. Yuan, Lagrangian coherent structures and mixing in two-dimensional turbulence. *Physica D* **147**, 352–370 (2000).

56. A. Scott, A nonlinear Klein-Gordon equation. *American Journal of Physics* **37**, 52–61 (1969).

57. D. Branford, O. C. O. Dahlsten, A. J. P. Garner, On defining the Hamiltonian beyond quantum theory. *arXiv [quant-ph]* (2018).

58. J. Rogel-Salazar, The Gross-Pitaevskii Equation and Bose-Einstein condensates. *arXiv [cond-mat.quant-gas]* (2013).

59. F. Wilczek, Quantum field theory. *Rev. Mod. Phys.* **71**, S85–S95 (1999).

60. W. Pauli, Pauli exclusion principle. *Naturwiss. Unterr. Chem.* (1924).

61. I. Haouam, On the three-dimensional Pauli equation in noncommutative phase-space. *arXiv [math-ph]* (2020).

62. S. Sarkar, On the trace of the product of Pauli matrices occurring asa r =a r i ? i +ia r 4 and that of the product of dirac matrices, and the interconnection between them. *Int. J. Theor. Phys.* **8**, 171–178 (1973).

63. N. Robotti, M. Badino, Max Planck and the "constants of nature." *Ann. Sci.* **58**, 137–162 (2001).

64. M. E. Shulman, Others, On the structure of electrons and other charged leptons. *J. High Energy Phys. Gravit. Cosmol.* **3**, 503 (2017).

65. A. N. Taylor, M. Rowan-Robinson, The spectrum of cosmological density fluctuations and nature of dark matter. *Nature* **359**, 396–399 (1992).

66. J. E. Forero-Romero, Y. Hoffman, S. Gottlöber, A. Klypin, G. Yepes, A dynamical classification of the cosmic web. *Mon. Not. R. Astron. Soc.* **396**, 1815–1824 (2009).

67. C. Becker, *et al.*, Oscillations and interactions of dark and dark-bright solitons in Bose-Einstein condensates. *arXiv [cond-mat.other]* (2008).

68. B. J. Carr, S. W. Hawking, Black holes in the early universe. *Mon. Not. R. Astron. Soc.* **168**, 399–415 (1974).

69. M. D. Smith, *The origin of stars* (World Scientific Publishing Company, 2004).

70. I. V. Barashenkov, A. D. Gocheva, V. G. Makhankov, I. V. Puzynin, Stability of the soliton-like "bubbles." *Physica D* **34**, 240–254 (1989).

71. K. Strecker, G. Partridge, A. Truscott, R. Hulet, Formation and propagation of matter-wave soliton trains. *Nature* **417**, 150–153 (2002).

72. D. An, T. C. Beers, Y. S. Lee, T. Masseron, A blueprint for the Milky Way's stellar populations. IV. A string of pearls—the galactic starburst sequence. *Astrophys. J.* **952**, 66 (2023).

73. T. Johannsen, Photon rings around Kerr and Kerr-like black holes. *The Astrophysical Journal* **777** (2013).

74. A. Ricarte, D. C. M. Palumbo, R. Narayan, F. Roelofs, R. Emami, Observational signatures of frame dragging in strong gravity. *Astrophys. J. Lett.* **941**, L12 (2022).

75. A. Ori, Structure of the singularity inside a realistic rotating black hole. *Phys. Rev. Lett.* **68**, 2117–2120 (1992).

76. A. Kravtsov, S. Borgani, Formation of Galaxy Clusters. *arXiv [astro-ph.CO]* (2012).

77. E. A. Yuzbashyan, Normal and anomalous solitons in the theory of dynamical Cooper pairing. *arXiv [cond-mat.supr-con]* (2008).

78. R. P. Feynman, Quantum electrodynamics. **3** (1998).

79. P. Wölfle, Quasiparticles in condensed matter systems. *Reports on Progress in Physics* **81** (2018).

80. A. Sommerfeld, The fine structure of Hydrogen and Hydrogen-like lines: Presented at the meeting on 8 January 1916. *Eur. Phys. J. H* **39**, 179–204 (2014).

81. J. Léonard, *et al.*, Realization of a fractional quantum Hall state with ultracold atoms. *arXiv [cond-mat.quant-gas]* (2022).

82. S. D. Bass, The spin structure of the proton. *Reviews of Modern Physics* (2005). https://doi.org/10.1103/RevModPhys.77.1257.

83. H. Harari, The structure of quarks and leptons. *Sci. Am.* **248**, 56–68 (1983).

84. U. R. Fischer, G. Baym, Vortex states of rapidly rotating dilute Bose-Einstein condensates. *Phys. Rev. Lett.* **90**, 140402 (2003).

85. V. Gribov, The theory of quark confinement. *Eur. Phys. J. C Part. Fields* **10**, 91–105 (1999).

86. M. Ferraris, M. M. Giannini, M. Pizzo, E. Santopinto, A three-body force model for the baryon spectrum. *Phys. Lett. A* (1995).

87. M. Oka, K. Yazaki, Nuclear Force in a Quark Model. *Physics Letters B* **90**, 41–44 (1980).

88. J. Ellis, The discovery of the gluon. *arXiv [hep-ph]* (2014).

89. W. Marciano, H. Pagels, Quantum chromodynamics. *Phys. Rep.* (1978).

90. G. W. Rayfield, F. Reif, Quantized vortex rings in superfluid helium. *Physical Review* (1964). https://doi.org/10.1103/PhysRev.136.A1194.

91. N. Feather, A survey of neutron and proton binding energies. *Adv. Phys.* **2**, 141–184 (1953).

92. R. Alonso, E. E. Jenkins, A. V. Manohar, A geometric formulation of Higgs Effective Field Theory: Measuring the curvature of scalar field space. *Phys. Lett. B* **754**, 335–342 (2016).

93. B. Horn, The Higgs field and early universe cosmology: A (brief) review. *Physics (College Park Md.)* (2020). https://doi.org/10.3390/PHYSICS2030028.

94. A. S. Wightman, Quantum field theory in terms of vacuum expectation values. *Phys. Rev.* **101**, 860–866 (1956).

95. M. Consoli, L. Cosmai, Spontaneous Symmetry Breaking and its pattern of scales. *Symmetry (Basel)* **12**, 2037 (2020).

96. A. Djouadi, J. I. Illana, Steven Weinberg and Higgs physics. *Nucl. Phys. B.* **1004**, 116541 (2024).

97. M. J. Gotay, J. E. Marsden, Stress-energy-momentum tensors and the Belinfante-Rosenfeld formula.

98. L. M. Brown, Hideki Yukawa and the meson theory. *Phys. Today* (1986).

99. A. Banerjee, G. Bhattacharyya, Probing the Higgs boson through Yukawa force. *Nucl. Phys. B.* **961**, 115261 (2020).

100. C. Csáki, C. Grojean, H. Murayama, Standard model Higgs boson from higher dimensional gauge fields. *Phys. Rev. D Part. Fields* **67** (2003).

101. J. M. Cornwall, Center vortices and confinement versus screening. *Physical Review D* (1998). https://doi.org/10.1103/PhysRevD.57.7589.

102. J. Harada, Roton energy gap and spontaneous symmetry breaking. *arXiv [cond-mat.other]* (2009).

103. A. B. Balantekin, B. Kayser, On the properties of neutrinos. *arXiv [hep-ph]* (2018).

104. J. Gratus, Y. N. Obukhov, R. W. Tucker, Conservation laws and stress-energy-momentum tensors for systems with background fields. *arXiv [physics.class-ph]* (2012).

105. P. J. E. Peebles, *et al.*, The case for the relativistic hot Big Bang cosmology. *Nature* **352**, 769–776 (1991).

106. R. Khatri, R. A. Sunyaev, Creation of the CMB spectrum: precise analytic solutions for the blackbody photosphere. *arXiv [astro-ph.CO]* (2012).

107. A. Labatie, J. L. Starck, M. Lachièze-Rey, DETECTING BARYON ACOUSTIC OSCILLATIONS. *Astrophys. J.* **746**, 172 (2012).

108. A. H. Guth, Inflationary universe: A possible solution to the horizon and flatness problems. *Physical Review D* (1981). https://doi.org/10.1103/PhysRevD.23.347.

109. R. Desbuquois, *et al.*, Superfluid behaviour of a two-dimensional Bose gas. *Nature Physics* **8**, 645–648 (2012).

110. A. Tononi, A. Cappellaro, G. Bighin, L. Salasnich, Propagation of first and second sound in a two-dimensional Fermi superfluid. *arXiv [cond-mat.quant-gas]* (2020).

111. L. V. Hau, S. E. Harris, Z. Dutton, C. H. Behroozi, Light speed reduction to 17 metres per second in an ultracold atomic gas. *Nature* **397**, 594–598 (1999).

112. Z. Dutton, M. Budde, C. Slowe, L. V. Hau, Observation of quantum shock waves created with ultra- compressed slow light pulses in a Bose-Einstein condensate. *Science* **293**, 663–668 (2001).

113. G. Dvali, M. S. Turner, Dark energy as a modification of the Friedmann equation. *arXiv [astro-ph]* (2003).

114. T. Padmanabhan, Cosmological constant—the weight of the vacuum. *Phys. Rep.* (2003).

115. R. R. Caldwell, A phantom menace? Cosmological consequences of a dark energy component with super-negative equation of state. *Phys. Lett. B* **545**, 23–29 (2002).

116. E. H. Lieb, J. Yngvason, "A guide to entropy and the second law of thermodynamics" in *Statistical Mechanics*, (Springer Berlin Heidelberg, 1998), pp. 353–363.

117. J. K. Singh, R. Nagpal, A model of dark matter dark energy interaction with some cosmic consequences. *arXiv [gr-qc]* (2023).

118. M. Hutley, Interference (holographic) diffraction gratings. *Journal of Physics E: Scientific Instruments* **9**, 513–520 (1976).

119. A. Rebane, J. Feinberg, Time-resolved holography. *Nature* **351**, 378–380 (1991).

120. T. Kreis, Digital holographic interference-phase measurement using the Fourier-transform method. *Journal of The Optical Society of America A-optics Image Science and Vision* **3**, 847–855 (1986).

121. J. H. C. Forrington, Time Dilation Cosmology 2. *J. Mod. Phys.* (2024).

122. F. W. Hehl, Y. N. Obukhov, Conservation of energy-momentum of matter as the basis for the gauge theory of gravitation. *arXiv [gr-qc]* (2019).

123. J. Erdmenger, A.-L. Weigel, M. Gerbershagen, M. P. Heller, From complexity geometry to holographic spacetime. *Phys. Rev. D.* **108** (2023).

124. U. Lupo, Aspects of (quantum) field theory on curved spacetimes, particularly in the presence of boundaries. (2015).

125. M. Breinig, "Schrodinger Equation" in *Compendium of Quantum Physics*, (Springer Berlin Heidelberg, 2009), pp. 681–685.

126. M. Namiki, S. Pascazio, Wave-function collapse by measurement and its simulation. *Phys. Rev. A* **44**, 39–53 (1991).

127. V. Galymov, An overview of the searches for the violation of the Charge-Parity symmetry in the leptonic sector. *Symmetry (Basel)* **16**, 130 (2024).

128. B. Wang, C.-Y. Lin, D. Pavon, E. Abdalla, Thermodynamical description of the interaction between holographic dark energy and dark matter. *arXiv [hep-th]* (2007).

129. D. Perlis, Consciousness as self-function. *J. Conscious. Stud.* (1997).

130. M. Welker, What is creation? Rereading genesis 1 and 2. *Theol. Today* **48**, 56–71 (1991).

131. T. Nagel, "11. What is it like to be a bat?" in *The Language and Thought Series*, (Harvard University Press, 2014).

132. R. Kanai, N. Tsuchiya, Qualia. *Curr. Biol.* **22**, R392-6 (2012).

133. T. A. de Graaf, P.-J. Hsieh, A. T. Sack, The "correlates" in neural correlates of consciousness. *Neurosci. Biobehav. Rev.* **36**, 191–197 (2012).

134. S. S. Yeo, P. H. Chang, S. H. Jang, The ascending reticular activating system from pontine reticular formation to the thalamus in the human brain. *Front. Hum. Neurosci.* **7**, 416 (2013).

135. B. Merker, Consciousness without a cerebral cortex: a challenge for neuroscience and medicine. *Behav. Brain Sci.* **30**, 63–81; discussion 81-134 (2007).

136. S. Kwak, M. C. Chang, Impaired consciousness due to injury of the ascending reticular activating system in a patient with bilateral pontine infarction: A case report. *Transl. Neurosci.* **11**, 264–268 (2020).

137. M. Maldonato, "The ascending reticular activating system: The common root of consciousness and attention" in *Recent Advances of Neural Network Models and Applications*, Smart innovation, systems and technologies., (Springer International Publishing, 2014), pp. 333–344.